International Journal of Biological Macromolecules 253 (2023) 127100

Contents lists available at ScienceDirect

International Journal of Biological Macromolecules

journal homepage: www.elsevier.com/locate/ijbiomac

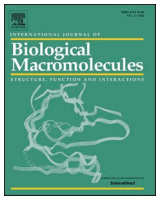

Understanding the intricacy of protein in hydrated deep eutectic solvent: Solvation dynamics, conformational fluctuation dynamics, and stability

Tanmoy Khan, Nilimesh Das, Kuldeep Singh Negi, Suman Bhowmik, Pratik Sen *

Department of Chemistry, Indian Institute of Technology Kanpur, Kanpur 208 016, UP, India

ARTICLE INFO

Keywords:
Deep eutectic solvent
Associated water dynamics
Conformational fluctuation dynamics

ABSTRACT

Deep eutectic solvents (DESs) are potential biocatalytic media due to their easy preparation, fine-tuneability, biocompatibility, and most importantly, due to their ability to keep protein stable and active. However, there are many unanswered questions and gaps in our knowledge about how proteins behave in these alternate media. Herein, we investigated solvation dynamics, conformational fluctuation dynamics, and stability of human serum albumin (HSA) in 0.5 Acetamide/0.3 Urea/0.2 Sorbitol (0.5Ac/0.3Ur/0.2Sor) DES of varying concentrations to understand the intricacy of protein behaviour in DES. Our result revealed a gradual decrease in the side-chain flexibility and thermal stability of HSA beyond 30 % DES. On the other hand, the associated water dynamics around domain-I of HSA decelerate only marginally with increasing DES content, although viscosity rises considerably. We propose that even though macroscopic solvent properties are altered, a protein feels only an aqueous type of environment in the presence of DES. This is probably the first experimental study to delineate the role of the associated water structure of the enzyme for maintaining its stability inside DES. Although considerable effort is necessary to generalize such claims, it might serve as the basis for understanding why proteins remain stable and active in DES.

1. Introduction

Enzymes are the most efficient and selective catalysts that play a significant role in diverse biochemical transformations and industrial processes [1–4]. However, the utilization of the enzymes is limited as they are only stable in water. Targeted enzyme mutation can overcome this issue to some extent [5–9]. Further, obtaining designer solvents that can keep enzymes stable and active is also very important for industrial applications [10–12]. Ionic liquids (ILs), owing to their non-volatility, high thermal stability, and a broad spectrum of solutes dissolving capabilities, become the most studied solvents in this regard [11,13–16]. More importantly, IL can be engineered by changing the constituent cations and anions [17,18]. However, in recent times, deep eutectic solvents (DESs) have been identified as the new choice for biocatalysis because of their additional advantages over ILs in terms of cost-effectiveness, easy (only through mixing and heating and no further purification required) and atom-economic preparation [19–21]. A huge number of naturally occurring/synthetic constituents and their different mole fractions can form DES, which provides a broad spectrum of engineered solvent media [22,23]. Many recent reports and review articles have highlighted that proteins remain stable and active in DES [24–30]. However, incorporation of proteins into neat DES is very difficult as their solubilization rate is extremely slow, and also incorporation through heating is inappropriate owing to the thermolabile character of proteins [31–33]. Adding water to the DES system in order to overcome this hindrance was found to be quite fruitful as it also offers an extra degree of freedom for tailoring solvent properties like viscosity and polarity that improves the dissolution rate of macromolecules [34,35]. More interestingly, the stability and activity of some enzymes are reported to get enhanced in hydrated DES media compared to that in the buffer [36–45]. This makes hydrated DES an exciting choice as a biocatalytic medium.

However, most of the research in this field relies on getting a positive result by choosing a pair of DES and protein. The choices are also getting biased on the availability of the proteins and DES constituents. A logical way forward in this field is very much missing. Nevertheless, some recent reports proposed that DESs properties like H-bond strength, interaction strength between DES constituents and protein, solvent polarity, viscosity, and density might influence the enzymatic activity and stability in such media [46,47]. Our group contributed to this

* Corresponding author.
E-mail address: psen@iitk.ac.in (P. Sen).

https://doi.org/10.1016/j.ijbiomac.2023.127100
Received 22 May 2023; Received in revised form 21 September 2023; Accepted 25 September 2023
Available online 29 September 2023

understanding by carrying out the proteolytic activity of bromelain in the presence of DES at various degrees of hydration [45]. We suggested that compact structural conformation, flexible active site dynamics of the enzyme; lower viscosity and higher polarity of the solvent media primarily affect the biocatalytic activity of bromelain [45].

However, the mechanistic understanding of why proteins/enzymes are stable and active in these alternate media (DES) is still in its infancy. One aspect that has been completely ignored in the literature is how the associated water dynamics of an enzyme is modulated in the presence of DES. It is well proven that the water in the immediate vicinity of an enzyme (known as associated water) is quite different from the normal bulk water [48–51]. This associated water is directly hydrogen bonded to the protein surface, making it dynamically retarded [48,49,51–53] and can influence many cellular processes [50,54–57]. The role of water dynamics in influencing protein properties has mainly been reported in the case of osmolytes [58–60]. Although there are some reports through MD simulation/theoretical studies in the case of different non-aqueous solvents pointing out the role of hydration [61–65], to the best of our knowledge there are no experimental studies in DES.

A variety of techniques are available to measure the dynamics of water, namely, NMR [66,67], dielectric relaxation (DR) [68], quasi-electron neutron scattering (QENS) [69], and time-dependent fluorescence Stokes shift (TDFSS) [50,53,55,56,70–74]. However, in the case of proteins, where the immediate surrounding is essential, the fluorescence-based TDFSS method becomes of utmost importance due to its unmatched spatial resolution [48,75]. It can report dynamics in the immediate vicinity of the reporter molecule tagged in the protein. In contrast, NMR, DR, or QENS captures signals from the whole solution and can give only an average picture [48]. In addition to associated water dynamics around the protein, internal protein dynamics is also a controlling factor of various cellular phenomena [76–81]. Among these, microsecond protein dynamics is one of the most important factors in controlling enzymatic activity and signal transduction. However, its modulation in DES is scarcely studied in the literature [45,47].

Herein, we aimed to understand the intricacy of protein behaviour in DES as a part of our ongoing effort to achieve a holistic physical insight into why proteins remain stable and active in DES. We have chosen human serum albumin (HSA) as a model protein that has been extensively characterized in the native state and under different conditions of chemical and thermal stress [13,70,82–85] and can be site selectively tagged to observe site-specific information [86,87]. HSA is the major transport protein in the human circulatory system [88], making the choice of HSA even more relevant. In the past, most of the experiments carried out to understand protein behaviour in DESs were done in ionic DESs [28,36,39,41,89,90]. However, for many practical purposes involving hydrophobic solutes, ionic DESs will not be a good choice. Non-ionic DESs can overcome this problem and in recent years such non-ionic DESs are gaining attention in various fields [91–93]. Therefore, understanding protein behaviour in non-ionic DESs is important. DES formed by acetamide, and urea is one of the most studied non-ionic DES [94,95], but it is not liquid at room temperature which limits its applicability [96]. We have reported earlier that adding sorbitol as a third component lowers the freezing point of the system [97]. This ternary DES with a composition of 0.5Ac/0.3Ur/0.2Sor remains in a liquid state even at 280 K. Because of this, we chose 0.5Ac/0.3Ur/0.2Sor DES for the present study.

In this work, we measured the solvation dynamics around the domain-I of HSA in 0.5Ac/0.3Ur/0.2Sor DES as a function of the degree of hydration using the TDFSS method. Analysis concerning individual components of solvation, water contents, and viscosity modulation is discussed, which might provide physical insight into enzymatic behaviour in DES. Secondly, we reported microsecond side-chain dynamics of domain-I of HSA with DES at various degrees of hydration. Thirdly, we have measured the thermal stability of HSA in the DES as a function of water content. More importantly, some control experiments with constituent solutions give us much-needed information regarding the retainment of DES structure with water dilution.

2. Experimental section

2.1. Materials

Acetamide, urea, sorbitol, human serum albumin (HSA), 7-diethylamino-3-(4'-maleimidylphenyl)-4-methylcoumarin (CPM), tetramethylrhodamine-5-maleimide (TMR), coumarin 343 (C343) and rhodamine 6G (R6G) were purchased from Sigma-Aldrich. Acetamide and urea were dried overnight under a vacuum at room temperature before use.

2.2. Tagging of protein

Cys-34 of HSA was covalently tagged to CPM and TMR following the previously described method [50,85]. Previously, our group and others used CPM and TMR to site-selectively tag HSA [82,85]. Briefly, two 10 ml, 90 μM stock solutions of HSA in the buffer of pH 7.4 were taken in round-bottom flasks. Separately each of the labeling dyes was prepared in DMSO and was added dropwise to one of the HSA solutions under stirring conditions such that in the final solution molar ratio became HSA: dye = 1:1.2. The reaction mixtures were then stirred for 12 h at 25 °C. Two reaction mixtures were then separately dialyzed against 1:20 (*V*/V) DMSO: buffer solution at 5 °C. The dialysis medium was changed 3 times a day for 4 days and then twice in 24 h till the complete removal of untagged dye (as measured by the absorption spectrum of the dialysis medium). The labeled proteins were concentrated using a 10 kDa centrifugal filtration unit. The site-selectivity of the tagging is confirmed through control experiments as described in section S1 of the Supplementary Material. Before doing any experiments with tagged protein, it is necessary to check if the tagging has perturbed protein structure. We proved that CPM and TMR tagging do not alter the secondary structure and thermal stability of HSA (see Fig. S2 and Table S1 of the Supplementary Material).

2.3. Acetamide-Urea-Sorbitol DES preparation

The DES was prepared by mixing the appropriate amount of the constituents in a sealed container to achieve the mole fractions as 0.5 Ac + 0.3 Ur + 0.2 Sor, and slowly heating to 75° C with stirring [45,98]. After one hour a clear solution of DES was obtained which remained liquid even at 280 K [45]. This DES was used for all the experiments. Precautions for external water incorporation were always taken care of.

2.4. Viscosity measurement

Dynamic viscosity of the sample was measured with a rolling-ball viscometer (Lovis 2000 M, Anton Paar, Austria) with an inbuilt temperature controller. The viscosity of the neat DES could not be measured at room temperature and was found to be ~482 cP at 45 °*C* [98].

2.5. Water content measurement

To determine the water content of DESs, we performed Karl Fisher titration (KAFI LABINDIA KF Titrator). For freshly prepared (from overnight vacuum-dried constituents) 0.5Ac/0.3Ur/0.2Sor DES, the water content is measured to be 0.3 % (*w*/w).

2.6. Steady-state absorption and emission

We performed the steady-state absorption and emission measurements in a commercial double-beam spectrophotometer (UV-2450, Shimadzu, Japan) and fluorimeter (FluoroMax-4, Jobin-Yvon, USA), respectively.

2.7. CD measurement

Circular dichroism spectra were recorded on a commercial CD spectrometer (J-815, Jasco, Japan) using a 2 mm path length cuvette, and the secondary structures were calculated using CDNN software [83,99].

2.8. Fluorescence correlation spectroscopy (FCS)

We performed fluorescence correlation spectroscopic (FCS) measurements on an instrument built in our laboratory. The setup and data analysis details can be found in our previous publications and section S2 of the Supplementary Material [76,78,98,100].

2.9. Time-resolved emission

Fluorescence transients of CPM-tagged HSA were measured in a picosecond time-correlated single-photon counting (TCSPC) setup (LifeSpec-II, Edinburgh Instruments, UK) under the magic angle (54.7°) condition. The excitation wavelength was 375 nm. The instrument response function (IRF) of the TCSPC setup is ~140 ps. Other details of this setup are described elsewhere [76,101,102]. The fluorescence transient was fitted and the average lifetime, $\langle \tau_{life} \rangle$, was estimated using eq. 1 [103]

$$I(t) = \sum_i a_i e^{\frac{-t}{\tau_i}}, \langle \tau_{life} \rangle = \sum_i a_i \tau_i \text{ with } \sum_i a_i = 1 \quad (1)$$

2.10. Solvation dynamics analysis

Solvation dynamics was analyzed using the time-dependent fluorescence Stokes shift (TDFSS) method by reconstructing the time-resolved emission spectrum (TRES) from the measured fluorescence transients of a solvatochromic fluorophore across the emission spectrum [104,105]. The process is based on the fact that when the probe is excited, the dipole moment changes significantly. This induces the rearrangement of the surrounding solvents to compensate for the change in the dipole moment of the probe, and a new equilibrium configuration is reached. The time taken for this solvent rearrangement is a measure of the solvation time [68,103]. We have recorded about 20 fluorescent transients across the steady-state emission spectrum of CPM tagged to HSA in the absence and presence of various DES concentrations. Subsequently, the normalized solvation response function was constructed as [103,105]

$$S(t) = \frac{\nu(t) - \nu(\infty)}{\nu(0) - \nu(\infty)} \quad (2)$$

where $\nu(t)$, $\nu(0)$, and $\nu(\infty)$ represent the emission maxima at time t, 0, and ∞, respectively. The average solvation time, $\langle \tau_s \rangle$, was obtained by fitting $S(t)$ to a multi-exponential function (Eq. 3) and taking the average of the decay time components as $\langle \tau_s \rangle = \sum_i b_i \tau_{si}$, where $\sum_i b_i = 1$.

$$S(t) = \sum_i b_i e^{\frac{-t}{\tau_{Si}}} \quad (3)$$

2.11. Solvation dynamics by Transient Absorption Spectroscopy (TA)

We used transient absorption (TA) spectroscopy to measure the solvation dynamics of the buffer and its modulation with DES addition. The detailed setup can be found in the previous publications [50,106]. Briefly, we used a commercial femtosecond TA spectrometer (Femto-Frame-II, IB Photonics, Bulgaria) for all the measurements. The laser system consisted of a mode-locked Ti:Sapphire femtosecond oscillator (MaiTai SP, Spectra-Physics, USA) and a Ti:Sapphire regenerative amplifier (SpitfirePro, Spectra-Physics, USA) pumped by a 20 W Q-switched Nd: zYLF laser (Empower, Spectra-Physics, USA). The regenerative amplifier generated 50-fs pulses at 800 nm with 4 mJ per pulse at a 1 kHz repetition rate. The fundamental beam is divided into two parts. One of them is used to generate the pump pulse after frequency doubling in a 0.2 mm β-barium borate (BBO) crystal. The other part is passed through a computer-controlled motorized delay stage and focused onto a 0.3 mm sapphire crystal to generate a white light continuum. All measurements are performed with a pump energy of 1 μJ, and the polarization of the pump was set at the magic angle (54.7°) to the probe pulse. Note that, complications might arise when the SE signal overlaps with another signal [107]. However, in the 450-550 nm spectral window, the difference absorption spectrum of coumarin 343 contains only stimulated emission. The time evolution of this stimulated emission signal is used to construct the solvent response function, $S(t)$, as described in eq. 2. The average solvation time, $\langle \tau_s \rangle$, was obtained by fitting $S(t)$ to a multi-exponential function (Eq. 3).

2.12. Sample preparation

All the samples were prepared in a phosphate buffer of pH 7.4 and kept overnight before measurement. Protein concentrations were kept at 5 μM, 4 μM, and 4 nM for steady-state/time-resolved fluorescence, CD, and FCS experiments, respectively. We have used a molar extinction coefficient of 36,500 M^{-1} cm^{-1} at 280 nm to determine HSA concentration [100].

3. Results and discussion

3.1. Hydrated DES or aqueous solution of DES constituents

There are debates in the literature on the preservation of the DES network in the presence of water [34,108–110]. Generally, for high water content, DES loses its typical structure and becomes a simple aqueous solution of the constituents [108–110]. Hence it is important to investigate if the hydrated DES in this study is merely an aqueous solution of its constituents. We separately prepared the hydrated DES solution and mixed all three constituents of DES in water maintaining the same component concentrations as in hydrated DES. From 70 % (v/v), the constituents were found to be insoluble in the required amount of water. This simple observation implies that from 70 % (v/v) onwards, DES in the water system is not merely an aqueous solution of the DES constituents, but rather a hydrated DES with the retention of the DES network. Next, we measured the translational diffusion of rhodamine 6G (R6G) in both the hydrated DES and aqueous solution of DES constituents using fluorescence correlation spectroscopy. All the raw data with fitting can be found in the supporting information (see fig. S4 of section S3 of the Supplementary Material). From the measured translational diffusion time we calculated microviscosity using the Stokes-Einstein equation.

Fig. 1 depicts that up to 30 % (v/v) DES in water, the microviscosity remains similar to that in the solution of constituents in water. However, from 30 % (v/v), a clear difference in the microviscosity of the hydrated DES and the component solution is visible. This experiment suggests that up to 30 % (v/v) DES in water, is probably an aqueous solution of the constituents of the DES. However, beyond that, it is surely a hydrated DES where the property cannot be achieved just by mixing the solution of DES constituents. We have earlier compared the proteolytic activity of bromelain in both hydrated 0.5Ac/0.3Ur/0.2Sor DES and aqueous component solution and observed a significant enhancement of activity at lower concentration (up to 40 % v/v) in the former case [45]. However, a slight increase in the proteolytic activity compared to pure buffer at lower concentrations of DES constituent solution was also observed [45]. Therefore, there is a hint that a synergistic action from the individual components might also play a role. Nevertheless, the significant positive effects on bromelain activity in hydrated DES probably arise due to the hydrogen-bonded network of the DES which might still exist even at such low concentrations of DES. Similar retention of the

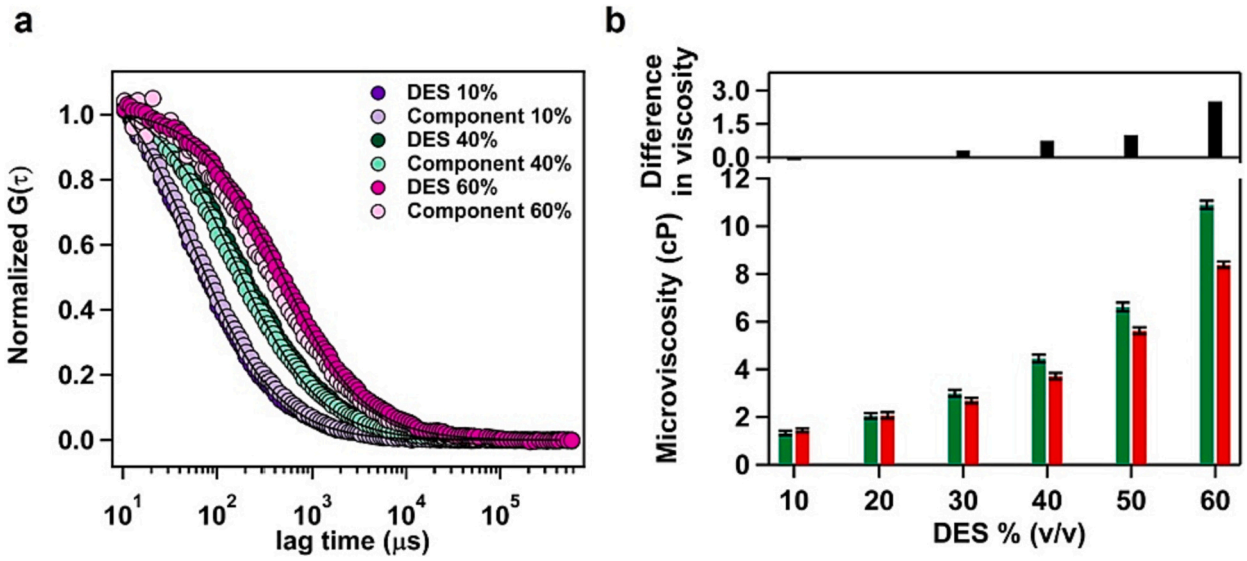

Fig. 1. (a) Representative fluorescence intensity autocorrelation curves of R6G in hydrated DES and component solution of the same concentration as in hydrated DES, (b) Micro viscosity of the hydrated DES (green) and constituent solution (red) keeping the same concentration as in hydrated DES. Black bars are representing the differences between the viscosity of hydrated DES and component solution. The error bar represents the standard deviation of the mean of three independent experiments.

network-like structure of choline chloride/urea and choline chloride/1,2-propane-di-ol DES was found up to 83 mol% and 50 % (v/v) of water, respectively [108,110]. Thus the structure retainment in the case of hydrated DES depends on the nature of the constituents. In our case, probably some portions of network-like DES structure maintain their integrity even at very low concentrations (~20-30 % v/v) of DES [45].

3.2. Solvation dynamics of hydrated DES using transient absorption spectroscopy

It is well known that dynamics of solvent play a significant role in many chemical and biological processes. However, experimental studies on the solvation dynamics of hydrated DES are limited in the literature [111,112]. Having established that the properties of hydrated DES cannot be achieved just by mixing the solution of DES constituents (at least beyond 30 % v/v DES), we measured solvation dynamics at various concentrations of DES in water using solvatochromic coumarin 343 probe with femtosecond transient absorption spectroscopy in the absence of the protein. We could not go beyond 70 % (v/v) DES concentration as the data quality becomes very poor due to scattering in the sample. The time-resolved stimulated emission spectra for different concentrations of DESs can be found in the section S4 of the Supplementary Material. From the collected data we constructed the solvent response function (see Fig. 2a) using eq. 2. The solvent response functions were well described by a bi-exponential function yielding the faster and the slower time components of solvation as 190 fs and 1.4 ps, respectively, in the case of buffer (Fig. 2c, d). We observed a gradual slowdown of solvation dynamics with increasing DES concentration (Fig. 2b). This is expected as the viscosity increases with the addition of DES in water (Fig. 2e). However, the faster time component remains almost unchanged. We have quantified the extent of this viscosity dependence of solvation dynamics (τ_s) using Stoke-Einstein relation as

$$\tau_s \propto \left(\frac{\eta}{T}\right)^p \tag{4}$$

where, η is the viscosity and T is the temperature of the medium [113]. p value signifies the coupling of the dynamics to the viscosity of the medium [114,115], which can be readily obtained from the log-log plot, as per eq. 5.

$$log(\tau_x) = plog\left(\frac{\eta}{T}\right) + logC \tag{5}$$

Expectedly, the average solvation time follows the medium viscosity (p ~ 1). Component analysis reveals that the slower component of solvation is also viscosity coupled (p ~ 1). However, the faster time component remains almost unchanged (p ~ 0). (Fig. 2c, f, and Table S2).

This result suggests that a bulk water-like ambiance around the probe might still exist even in the presence of 70 % (v/v) DES, where the viscosity is very high. At the same time, the addition of DES to the buffer significantly alters medium properties (like microviscosity, average solvation time, etc.). The impact of this result can be extended in the case of protein where the immediate water near the protein surface which is in direct interaction with the protein can influence many important enzymatic properties like stability and activity [53,55,56]. We hypothesized that although biological observations are always system-specific, one general way of keeping protein stable and active in viscous DES might be through retaining this unperturbed portion of water around it.

3.3. Associated water dynamics of HSA with increasing DES content

To understand the associated water dynamics around the protein, we measured the solvation dynamics of CPM tagged to HSA in buffer, and in the presence of different concentrations of 0.5Ac/0.3Ur/0.2Sor DES. All the relevant data is shown in Fig. 3 and also tabulated in Table 1. Time-resolved emission spectra (TRESs) are shown in fig. S6 of section S5 of the Supplementary Material. The average solvation time of CPM-tagged HSA in water is ~2.2 ns, which gradually increases upon the addition of DES and becomes ~3.4 ns for 90 % (v/v) DES in water. Initially, we thought that it might be a direct/straightforward consequence of increasing medium viscosity with increasing DES concentration. However, the viscosity change for the 90 % DES is ~83 times (from ~1 cP in water to ~83 cP in 90 % DES) (see Fig. 2e). Therefore, the extent of the increase in the solvation time with increasing DES concentration is negligible compared to that of the viscosity increment. It hints that HSA can maintain the associated water structure around it even in the presence of high concentrations of DES.

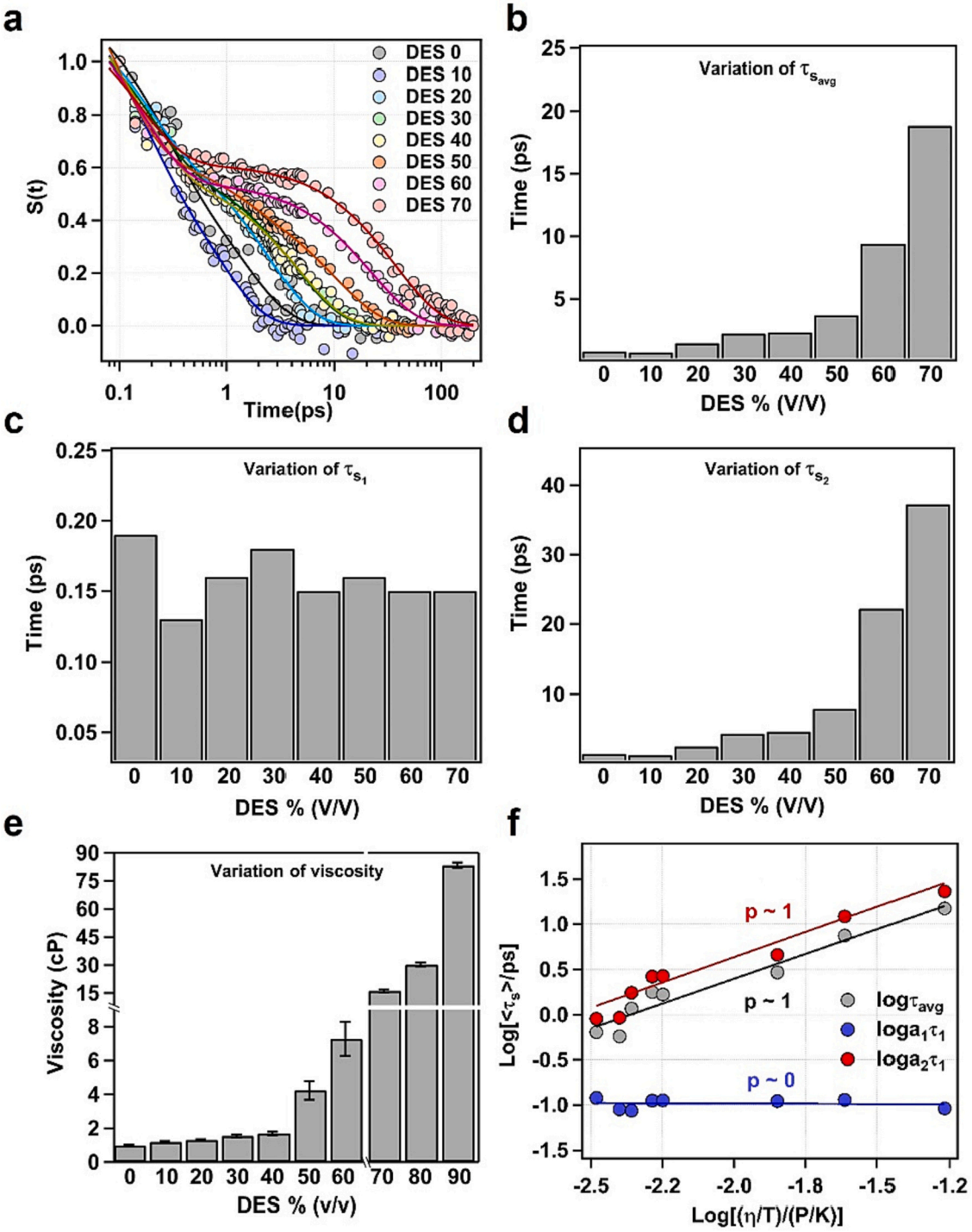

Fig. 2. (a) Solvent response function of C 343; and variation of (b) average solvation times, (c) faster time components, (d) slower time components with different degrees of hydrated 0.5Ac\0.3Ur\0.2Sor DES in the absence of protein, (e) viscosity of different concentrations of 0.5Ac/0.3Ur/0.2Sor DES in the buffer, (f) log-log plot of individual timescales of solvation dynamics of hydrated 0.5Ac\0.3Ur\0.2Sor DES with the temperature reduced viscosity.

3.4. Component analysis suggests first solvation shell remains unperturbed with DES

A deeper insight could be gained from the individual component analysis. In the experimental result, the bi-exponential solvent response functions were comprised of a sub-nanosecond (130-250 ps) and a few nanoseconds (3-5 ns) time components. The faster sub-nanosecond time component originates from the water molecules residing in the immediate vicinity of the protein surface, commonly termed biological water [49,51,53,116,117]. The longer timescale represents the contribution from polar residues of the protein, coupled motion between the amino acid side-chain fluctuations and water molecules, and the overall tumbling motion of the protein [48,49,51,117]. The variation of faster (τ_{S_1}) and slower (τ_{S_2}) time components of solvation are represented in Fig. 4a and Fig. 4b. Like in the case of solvation dynamics of hydrated DES in the absence of protein, here also the faster time component remains unaltered up to 70 % DES. It suggests an unperturbed first solvation shell around HSA up to 70 % DES. Beyond that the associated water dynamics

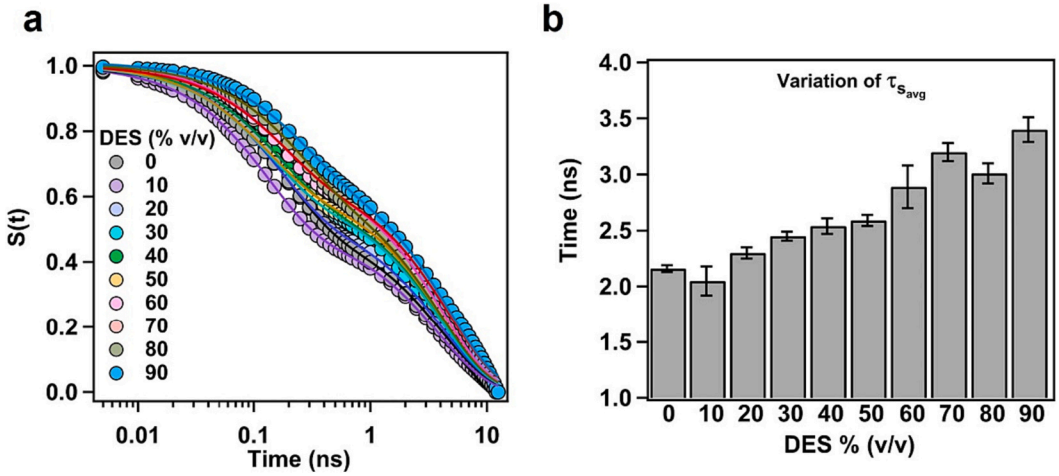

Fig. 3. (a) Solvent response function and (b) average solvation time of CPM labeled HSA in buffer and different concentrations of 0.5Ac/0.3Ur/0.2Sor DES. The error bar represents the standard deviation of the mean of three independent experiments.

Table 1
Biexponential fitting parameters of the solvent response function, S(t), of CPM, tagged HSA in the presence of different concentrations of 0.5Ac/0.3Ur/0.2Sor DES and the viscosity of different concentrations of 0.5Ac/0.3Ur/0.2Sor DES in the buffer.

DES concentration %(*V*/V)	a_1	τ_{S_1} (ps)	a_2	τ_{S_2} (ns)	$\tau_{S_{avg}}$ (ns)	Viscosity (cP)
0	0.49	170±10	0.51	4.08±0.10	2.16±0.03	0.98±0.04
10	0.51	160±15	0.49	4.02±0.24	2.05±0.13	1.19±0.05
20	0.46	160±10	0.54	4.13±0.22	2.30±0.05	1.31±0.04
30	0.40	130±20	0.60	4.00±0.10	2.45±0.04	1.54±0.08
40	0.40	150±10	0.60	4.14±0.17	2.54±0.07	1.68±0.10
50	0.38	130±20	0.62	4.09±0.10	2.58±0.05	4.23±0.55
60	0.34	160±10	0.66	4.29±0.10	2.89±0.19	7.27±1.00
70	0.33	170±10	0.67	4.68±0.15	3.20±0.08	16.14±0.80
80	0.37	230±20	0.63	4.65±0.20	3.01±0.09	30.16±1.00
90	0.31	250±20	0.69	4.81±0.22	3.40±0.11	83.30±1.50

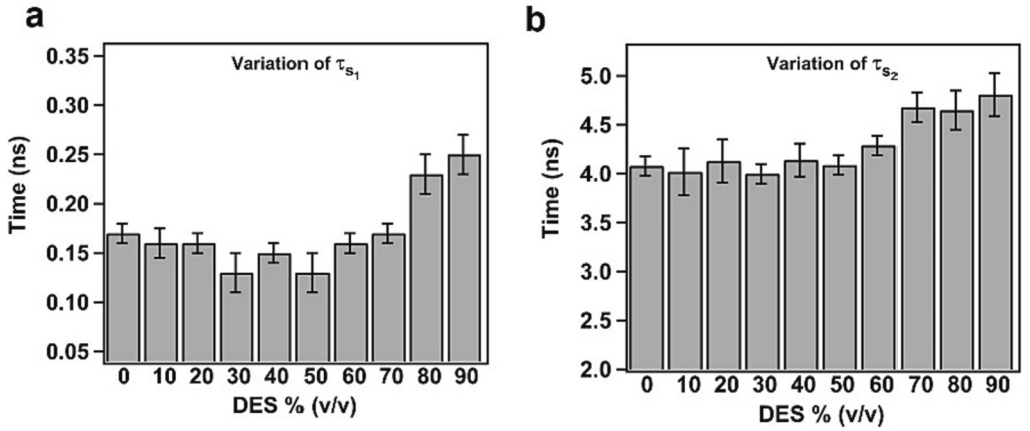

Fig. 4. The variation of (a) faster time component and (b) slower time component of CPM tagged HSA in the presence of different concentrations of 0.5Ac/0.3Ur/0.2Sor DES in the buffer. The error bar represents the standard deviation of the mean of at least two independent experiments.

slightly gets affected. However, these changes are also insignificant concerning the significant viscosity change of the medium.

To quantify how much the solvation dynamics and its individual components are coupled to the viscosity of the medium, here also we have constructed the log-log plot (see Fig. 5). The slope of the log-log plot for the fast component is almost zero, implying this to be viscosity independent. This means that the associated water dynamics around the protein is not modulated at all with the addition of DES. The slow component also shows a very weak viscosity coupling.

This result is remarkable. It suggests that at least in the first solvation shell, water structure is maintained at least up to 70 % (v/v) of DES. Protein, therefore, feels only an aqueous environment, even at this concentration of DES, where the macroscopic properties of the system, like viscosity, change drastically (up to 16 times at 70 % DES). It is almost axiomatic that water plays an important role in dictating every protein property. Especially, the associated water, that directly interacts with a protein, should have a huge effect on protein properties [48,50,53,55]. Our result implies that the character of this associated water remains unperturbed in the presence of DES. It might have an enormous implication in the field of biocatalysis and provides a clue that

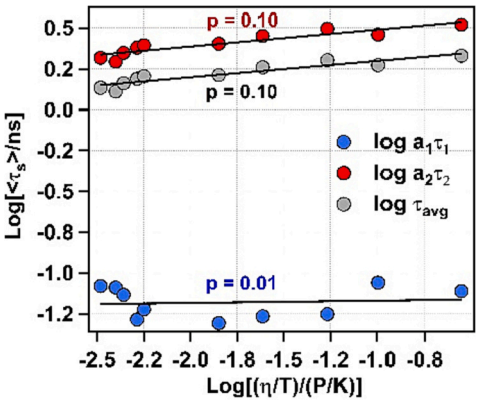

Fig. 5. Log-log plot of individual timescales and average solvation time of CPM labeled HSA with the temperature-reduced viscosity of different concentrations of 0.5Ac/0.3Ur/0.2Sor DES in the buffer.

enzymes remain active and stable in DES by keeping its associated water structure intact. Previously, Hayyan's group suggested a similar mechanism to explain the stability and activity of an enzyme in the DES using MD simulation [29]. Our findings likely represent the first experimental support in favour of such a mechanism.

3.5. Solvation dynamics of HSA in component solution

We also measured solvation dynamics of HSA in the aqueous solutions of DES constituents and compared the results with hydrated DES. All the time resolved emission spectra (TRESs) can be found in section S6 of the Supplementary Material. As the microviscosity (Fig. 1b) in the case of hydrated DES is more than the same concentration of aqueous solution of constituents, the dynamics are expected to be affected less in the latter case compared to the former. We observed a monotonous slowing down of solvation dynamics with an increase in the constituent concentration, though the faster time component, which represents the associated water dynamics around HSA, remains unaltered (Fig. 6 and Table 2). The extent of slowing down in the solvation dynamics is almost

Table 2
Biexponential fitting parameters of the solvent response function, S(t) of CPM, tagged HSA in the presence of different concentrations of constituent solution of 0.5Ac/0.3Ur/0.2Sor DES.

DES concentration %(V/V)	a_1	τ_{S_1} (ps)	a_2	τ_{S_2} (ns)	$\tau_{S_{avg}}$ (ns)
0	0.49	170±10	0.51	4.08±0.10	2.16±0.03
10	0.50	140±15	0.50	4.11±0.16	2.12±0.02
20	0.47	160±10	0.53	4.17±0.11	2.28±0.02
30	0.46	160±15	0.54	4.20±0.09	2.34±0.09
40	0.46	170±15	0.54	4.25±0.08	2.37±0.04
50	0.40	140±10	0.60	4.00±0.09	2.45±0.05
60	0.34	155±20	0.66	4.37±0.16	2.94±0.03

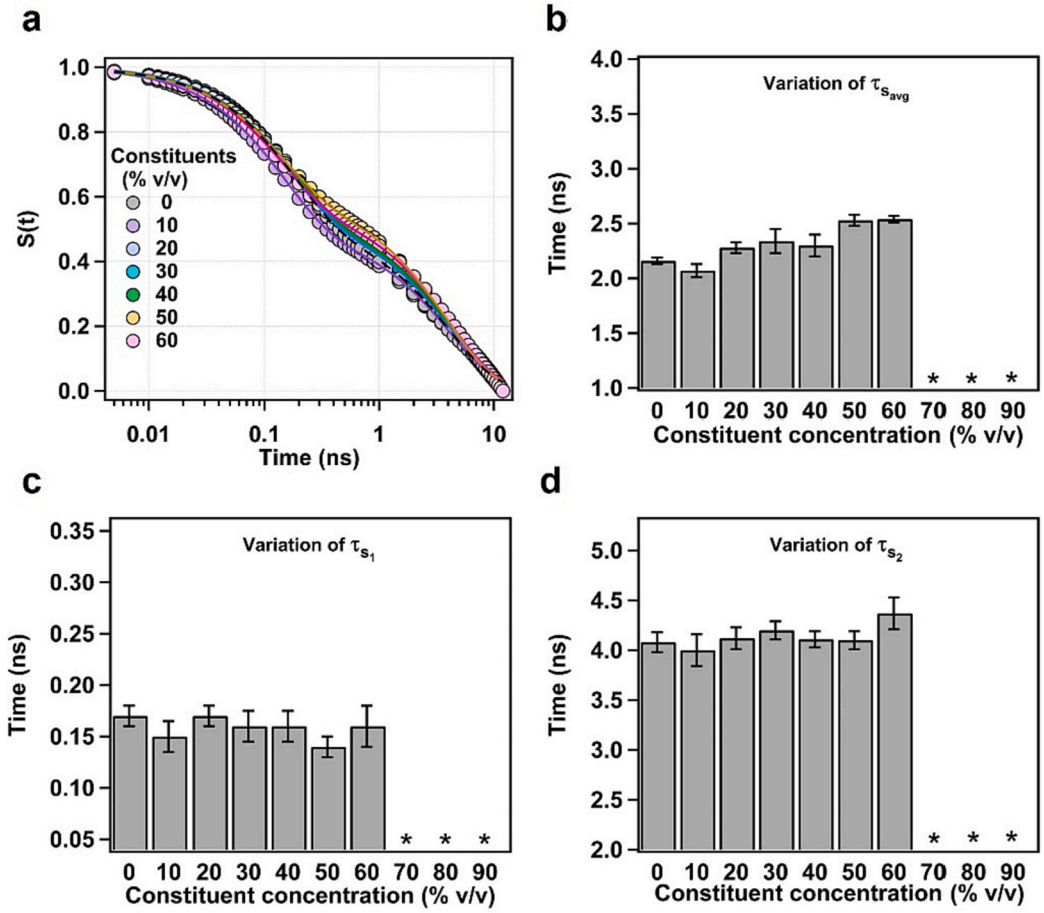

Fig. 6. (a) Solvent response function, (b)variation of average solvation time, (c) variation of faster time component and (d) variation of the slower time component of CPM tagged HSA in the presence of buffer and different concentrations of constituent's solution of 0.5Ac/0.3Ur/0.2Sor DES. Solid lines in (a) represent fitting by eq. 3. "* (Asterix)" points could not be measured as the constituents remain insoluble at those concentrations. The error bar represents the standard deviation of the mean of at least two independent experiments.

similar to that in hydrated DES. This observation is very surprising considering that at least above 30 % (v/v) hydrated DES is different from the aqueous solution of DES components in terms of macroscopic and microscopic properties (Section 3.1.).

We propose that DES or hydrated DES keep protein stable and active by maintaining the associated water around it and at the same time providing an alternate media where the physical properties can be fine-tuned as per the requirement. Proteins also remain stable and active in the presence of various osmolytes, ILs, and macromolecular crowders. In a previous report, we have shown that associated water dynamics play a key role in controlling protein stability in the crowded milieu [50]. We suggest that associated water property might be one of the principal governing factors in controlling protein behaviour in the presence of any additives.

3.6. Protein structural modulation and solvation dynamics

One may debate whether the constancy of solvation dynamics results merely from the conservation of the HSA's associated water structure in the presence of DES or whether the water structure and protein structure are regulated to keep the solvation dynamics constant. When a protein changes its conformation or structure, the bulk water molecules are expected to interact with the hydration layer to a different extent, resulting in a change in the solvation dynamics. To investigate if such an alteration plays a key role in the modulation of solvation dynamics, we performed a steady-state emission study of CPM attached to HSA that provides the local environment around it and estimated the hydrodynamic radii of HSA with the addition of DES using FCS. We also presented previously reported changes in the emission maximum and hydrodynamic size of CPM-tagged to HSA with the addition of guanidinium hydrochloride (GnHCl) [85,87], as a control to understand the extent of change in the presence of DES. GnHCl is a common denaturing agent and with an increase in the concentration, it destabilizes the native conformation of any protein [118]. The effect of GnHCl-induced denaturation of HSA is well reported in the literature by various groups including ours [83–85,87,119,120]. The change in the emission maximum and hydrodynamic radius with GnHCl concentration is plotted here to show the extent of the effect exerted by DES on the structure of HSA in comparison to a common denaturing agent, which is supposed to unfold the protein. Our experiment shows almost no shift in the emission spectrum in the presence of different concentrations of DES (Fig. 7a and Table 3). Also, there is virtually no change in the hydrodynamic radii of HSA up to 30 % of DES. However, beyond that, the size of the protein increases with an increase in the DES content of the medium (Fig. 7b and Table 3). The emission and FCS-related raw data can be found in figs. S8 and S9 of section S7 of the Supplementary Material. This increase in the size of HSA suggests a disruption of HSA structure with the addition of DES, although the change is not much (39 Å in the buffer to 49 Å in 80 % DES) compared to the chemical denaturation (63 Å in 6 M GnHCl). This means although the hydrodynamic radius of HSA starts to increase around 40 % (v/v) DES, it surely does not reach the completely unfolded state even in the presence of the highest concentration of the DES used here.

Obviously, the alteration of protein conformation at the higher DES concentration might affect its solvation dynamics. However, when a protein opens up due to its structural alterations, more bulk water molecules are expected to interact with the hydration layer of the protein surface, thus will accelerate the process [87,121]. On the other hand, for higher DES concentrations the water dynamics in the present case did not speed up. This suggests that despite a slight but definitive structural alteration, it does not severely affect the water structure modulation.

Table 3
Steady-state emission maxima of CPM-tagged HSA, hydrodynamic radii (see Supplementary Material for calculation), and conformational fluctuation time of TMR-tagged HSA in different concentrations of 0.5Ac/0.3Ur/0.2Sor DES in buffer.

DES concentration (% *V*/V)	Emission maxima (nm)	Hydrodynamic radii (Å)	Conformational fluctuation time (τ_R) (μs)
0	463.0± 1.0	38.2±2.6	27.0±6.6
5	462.8±0.7	36.6±2.6	32.4±3.7
10	462.8±0.6	36.5±1.9	32.0±4.8
15	462.6±0.6	36.4±1.8	36.0±7.9
20	461.9±0.7	36.0±2.0	31.8±6.7
25	461.8±0.8	37.8±3.5	34.0±5.1
30	462.2±0.5	40.4±3.1	29.0±6.9
35	462.3±0.6	42.9±3.0	32.0±7.2
40	462.3±0.9	46.0±2.6	45.0±9.1
45	462.1±0.8	46.5±3.4	60.0±10.4
50	462.5±1.0	46.8±2.9	71.0±9.6
55	462.4±0.5	47.1±3.6	80.0±7.0
60	462.3±0.6	47.0±3.0	85.0±9.7
65	462.0±0.7	47.2±2.8	90.0±6.3
70	461.8±0.7	47.5±3.3	95.0±7.9
80	461.3±1.0	49.0±3.5	110±10.0
90	461.0±0.8	*	*

* We could not measure the hydrodynamic radius and τ_R at 90 % DES, as the data quality of HSA becomes very poor at this concentration.

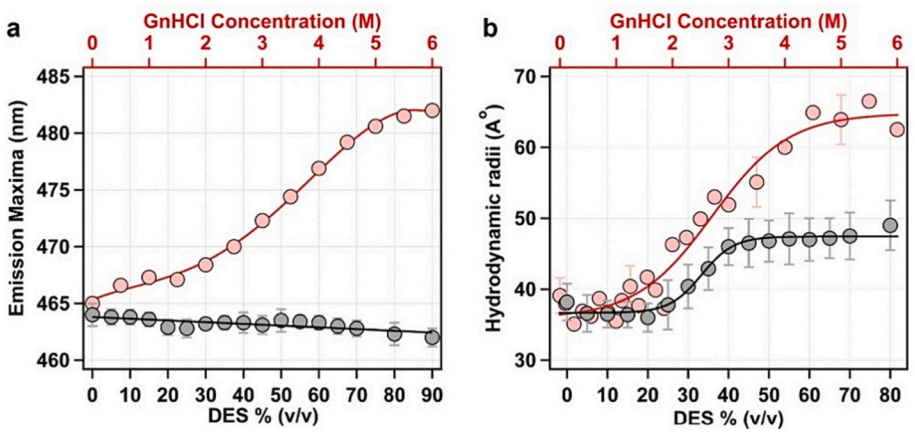

Fig. 7. (a) Steady-state emission maxima of CPM labeled HSA in different concentrations of 0.5Ac/0.3Ur/0.2Sor DES in buffer (grey). (b) Hydrodynamic radius of HSA with DES concentrations (grey). The data points shown in red have been taken from REF- [85] and [87] and represent the emission maxima and hydrodynamic radius with GnHCl concentration in the respective figures. The error bar represents the standard deviation of the mean of three independent experiments.

3.7. Conformational fluctuation of HSA in the presence of DES

Besides the water dynamics, the intrinsic protein dynamics or conformational fluctuation dynamics can also play a role in dictating protein properties [76,77,79,80]. It is well-accepted that the protein structure is not rigid, instead, it is an average of several closely related structural conformations [122]. The interconversion timescale between these conformations is known as conformational fluctuation time. Many studies confirmed the role of such inherent dynamics on enzymatic activity [77,80,122,123]. Experimentally the conformational fluctuation dynamics of proteins in the presence of DES have not been explored in detail. There are few studies of the conformational fluctuation dynamics of proteins in ILs [13,124], but probably only one or two studies reported the conformational dynamics of a protein in the case of DES [47,125]. In our previous work, we correlated the flexible active site dynamics of bromelain to the superior proteolytic activity in the presence of a DES [45].

For the present case, we also have analyzed the conformational fluctuation dynamics from the FCS autocorrelation function (see figs. S3 and S9 of the Supplementary Material). This fluctuation is a very local phenomenon and represents the ease of the concerted chain motion dynamics [84,85,126]. Because of this dynamics, the electron-rich amino acid residues around TMR (tagged in the domain-1 of HSA) move close and away from the probe, thus modulating its fluorescence behaviour, and can be observed in the single molecular level FCS experiment [82,85]. In the buffer, the measured value of conformational fluctuation time is 27 μs, which is following the previous report [85]. With the addition of DES, the conformational fluctuation dynamics become progressively slower (see Fig. 8 and Table 3), significantly beyond ~30 % DES. There could be various reasons for such modulations. Firstly, with increasing DES concentration, the viscosity of the medium increases, and this increased friction might slow down the side chain dynamics. However, the extent of slowing down of conformational dynamics involving domain-1 of HSA (~4 times) is much less than the increment of viscosity (~30 times) as we move from buffer to 80 % DES. Secondly, the size of HSA increases (especially beyond 30 % DES), so the surrounding electron-rich residues that quench TMR fluorescence now need to move a greater distance, and it might increase the timescale of such movement. However, in our previous publications, we showed that such a relationship between protein size and conformational time scale might not always hold [78,100,127]. At this stage, it is tough to predict the exact reason for such a trend, but it might have a key implication on its behaviour [77,128]. To note, a similar modulation of conformational flexibility was observed for another protein: bromelain in the same DES [45].

The conformational fluctuation dynamics and solvation dynamics are two very different information about protein and its surrounding solvent, respectively. Obviously, the internal protein dynamics depend on the rigidity of the surrounding solvent (associated water) and therefore there might be a correlation between them. Previously, a correlation has been established between internal protein dynamics in nanosecond timescale and solvation dynamics [129]. However, the correlation between microsecond conformational fluctuation and solvation is not known. Apparently, the rigid associated water structure should hinder side-chain dynamics, therefore an increase in the conformational fluctuations time should be associated with an increase in solvation time. Our results also indicate the same. Up to 40 % DES, both parameters remain almost constant. However, beyond that there is an increase in both the solvation and conformational fluctuations time. Moreover, the dependence of conformational fluctuations on DES concentration (~ 4 times increment from 0 to 80 % DES) is much steeper than that of the solvation time (~1.5 times increment from 0 to 90 % DES). At this point, it is very difficult to ascertain the reason behind this. One possible explanation could be that both these parameters depend strongly on the protein structural modulation in the presence of DES. At higher DES concentrations, HSA is somewhat unfolded. For unfolded protein because the exchange channel between associated and bulk water increases, solvation time decreases. However, for unfolded protein, because the distance between the tagged dye and the neighbouring amino acids increases, the conformational fluctuations time might increase. Another possibility may lie in the time scale and length scale of the dynamics. Solvation dynamics occur in the sub-picosecond to the nanosecond time scale and in the sub-nanometre length scale, whereas conformational fluctuations occur in the microsecond time scale and nanometre length scale. This difference in the time and length scale of these two dynamics might respond to a perturbation (viscosity change for example) differently.

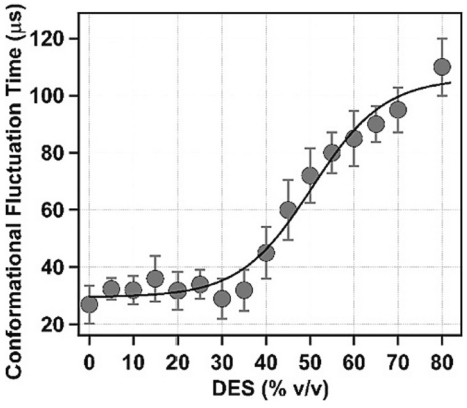

Fig. 8. The variation of conformational fluctuation time of HSA as a function of 0.5Ac/0.3Ur/0.2Sor DES concentration in the buffer. The error bar represents the standard deviation of the mean of three independent experiments.

3.8. Effect of DES content on the stability of HSA

Next, to understand the stability of HSA in the presence of DES, we have used steady-state fluorescence spectra of CPM-tagged HSA to obtain the melting curve of HSA (see Fig. 9) in the presence of different DES contents. Generally, with denaturation, the protein becomes unfolded, and as a signature, any solvatochromic probe attached to the

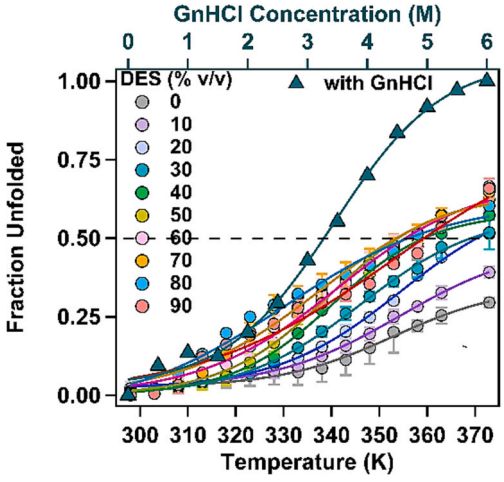

Fig. 9. Melting curves in terms of fraction unfolded of CPM-tagged HSA at different concentrations of 0.5Ac/0.3Ur/0.2Sor DES in the buffer. The solid lines are the eye guides. Note that emission maxima in the presence of 6 M GnHCl have been taken as the totally unfolded state in calculating fraction unfolded curves at each DES concentration. Variation of the fraction unfolded with increasing concentration of GnHCl (dark green) was plotted with respect to the similar colour-coded top axis (dark green). The error bar represents the standard deviation of the mean of three independent experiments.

protein shows a red shift in the emission maximum. All the steady-state fluorescence spectra are provided in section S8 of the Supplementary Material. From the shift of emission spectra, we have calculated the fraction unfolded at each temperature using the equation, $f_U = \frac{\lambda^{em} - \lambda_N^{em}}{\lambda_U^{em} - \lambda_N^{em}}$. In this equation, λ^{em} is the emission maxima of CPM-tagged HSA at any temperature; λ_N^{em} and λ_U^{em} are the emission maxima of the native and unfolded state of HSA, respectively. As the thermal unfolding curve of HSA was not saturating, choosing the unfolded state from those data is very difficult. However, the GnHCl-induced chemical denaturation curve of HSA shows a hint of saturation and reached a totally unfolded state at 6 M GnHCl. So, we constructed the normalized melting curves (fraction unfolded) at each degree of hydrated DES (Fig. 9), considering the lowest emission maxima as the native and the emission maxima of the 6 M GnHCl as the unfolded state of HSA. The temperature at which the fraction unfolded and folded becomes equal, i.e., fraction unfolded = 0.5, can be considered as melting temperature. However, we restrained ourselves from extracting any melting temperature or thermodynamic entity from these curves, as the curves do not get saturated and reached the plateau, even at the highest temperature (373 K) used in this study. From the melting curves (Fig. 9), one could conclude that at low concentrations of DES (up to 30 % (v/v)), the change in the stability is less, but beyond that, a significant decrease in the stability is observed. Such decreasing stability can be a direct consequence of structural alteration of the HSA at higher DES concentration. We have seen an increase in the hydrodynamic radius of the HSA beyond 30 % (v/v) of DES. However, at the lower DES concentration, where the structure remains unperturbed and associated water dynamics do not change much, DES retains most of the stability of HSA. At very high concentrations of DES (80-90 %) the associated water dynamics also slightly get perturbed along with the protein structure, which is probably responsible for the significant stability loss. Next, we also measured the thermal stability of HSA in the constituent aqueous solution keeping the concentrations of each of the constituents same as in hydrated DES. All the related raw data and the melting curves can be found in sections S9, and S10 of the supplementary material. We found that at lower concentration (up to 40 %) the thermal stability curves of HSA both in the hydrated DES and component solution matches well. However, after 40 % the stability is a little higher in the case of hydrated DES than in component solutions (see fig. S12 of section S10). Probably the network-like structure of DES, which surely exists in the higher DES concentrations, has some protective role towards HSA. Recently, we experimentally showed a strong correlation between protein stability and associated water structure modulation [50]. A pre-requisite of such correlation is that the added perturbation does not change the structure much. As this condition is not fulfilled in this case, any direct correlation of stability with associated water dynamics is not possible at this stage. In the future project, we will examine whether a correlation between stability and associated water structure holds good in DES medium.

4. Comparison of our results in the light of previous literature

The most thoroughly studied enzyme in DES is probably lipase [16,28–30,39–41,43,61,62,65,130]. The biocatalysis by lipase in DES has been first reported by Gorke et al. [39]. It was found that 12 % urea led to a loss of 70 % enzymatic activity of lipase. However, in choline chloride/urea (containing 66 % urea) DES merely less than 1 % of enzymatic activity is lost and the stability of the enzyme was found to be higher in the DES than in the corresponding component solution [39]. Monhemi et al. with the help of MD simulation pointed out that an alteration of hydrogen bonding of water with the protein surface might have a role in altering the enzyme stability and activity in such urea-based DES [65]. Durand et al. observed that the addition of up to 20 % water improves the lipase activity at least 10 times in choline chloride/urea DES [40]. However, in another study, Zhou et al. reported the deleterious effect of choline chloride/urea DES on *Candida antarctica* lipase B catalyzed epoxidation reaction, whereas choline chloride/sorbitol DES stood out as an efficient media for the same reaction [131]. These hints that activity and stability depend very much on the nature of protein and DES. Esquembre et al. were the first to examine the concentration effect of hydrated choline chloride/urea and choline chloride/glycerol DESs on hen egg lysozyme and found that aqueous dilution from the neat DES leads to refolding of the thermally denatured state of lysozyme and the activity was also recovered [36]. On the other hand, Zeng et al. reported refolding of thermally unfolded lysozyme with increasing betaine/urea DES concentration [132]. Various other experimental and simulation studies delineated the superiority of hydrated DES over neat DES [36–38,42–44,133,134]. There are few reports on bovine serum albumin (BSA) in urea-based DESs as well. The extraction efficiency of BSA in hydrated choline chloride/urea and betaine/urea DES was found to be more than in ILs and these DESs also keep the conformation of the protein intact [135]. However, the effect of neat DES on BSA was found to be detrimental [32]. Very recently, Venkatesu and co-workers have reported BSA in a solvent system comprised of macromolecular crowders and DES together. Interestingly the combination of choline chloride/urea with polyethylene glycol showed an elevated melting temperature of BSA than individual crowder or DES [136]. However, to the best of our knowledge, there is no report deciphering the enzymatic properties of HSA in any DES. Here we used a non-ionic DES (0.5Ac/0.3 Ur/ 0.2 Sor) at different degrees of hydration. Previously the structure, activity, and dynamics of proteolytic enzyme bromelain were reported in this same hydrated DES by our group [45]. We found that at all DES concentrations, enzymatic activity was retained. Moreover, at lower DES concentrations (up to 30 % v/v) the proteolytic activity even increases compared to that in buffer and then it decreases with a further increase in the DES concentration. In this report, we measured the solvation dynamics of HSA in the same hydrated DES. To the best of our knowledge, this is probably the first experimental report on the solvation dynamics of any protein in DES. We found that associated water around the protein does not alter up to 70 % v/v DES. We also found that the thermal stability of HSA does not change much up to 30 % DES and then decreases with increasing DES concentration. This study provides a clue that enzymes remain active and stable in DES by keeping their associated water structure intact. However, any direct correlation of stability with associated water dynamics is not possible at this stage because structural alteration of the HSA at higher DES concentration (beyond 30 %) can also influence the stability. An increment in protein hydrodynamic radius with DES addition was reported in the case of cellulase enzyme in the presence of ChCl-lactic acid DES [137]. Previously, Kist et al. also found a similar deleterious effect on the thermal stability of ribonuclease A with increasing concentration of choline chloride/urea DES [138]. Overall, the enzymatic property in DES depends on both the nature of DES constituents and proteins. Through this study, we want to emphasize considering associated water dynamics modulation in order to understand the protein behaviour in hydrated DES. Also, the associated water property might be one of the principal governing factors in controlling protein behaviour in the presence of any additives.

5. Overall understanding and conclusions

Herein, we contemplated the modulation of solvation dynamics/conformational fluctuation dynamics around domain-I of HSA and the thermal stability of HSA in 0.5Ac/0.3Ur/0.2Sor DES with varying degrees of hydration to understand the intricacy of protein behaviour in DES. Also, from control experiments, we proved that at least beyond 30 % (v/v) DES it is surely a hydrated DES, the properties of which cannot be achieved just by mixing the solution of DES constituents.

The main findings can be summarised as follows: (i) We have measured the solvation dynamics of the hydrated DES system in the absence of protein using transient absorption spectroscopy and found that the average solvation time follows the medium viscosity but a

portion of water remains bulk-like. (ii) Solvation dynamics around domain-I of HSA with increasing DES content slows down very slightly with respect to the huge viscosity increment (~83 times at 90 % DES). Component analysis of solvation dynamics suggests that the first solvation shell remains unperturbed at least up to 70 % DES. (iii) Although the mixture of individual components differs from hydrated DES in terms of microviscosity, the alteration of solvation dynamics of domain-I of HSA shows similar behaviour to that in hydrated DES. (iv) The microsecond conformational fluctuation dynamics of domain-I of HSA is unperturbed up to ~30 % DES, and beyond that, it becomes gradually slower. (v) The thermal stability of HSA gradually decreases with the addition of DES. The effect is more prominent in the DES constituent's solution than in the same concentration of hydrated DES. Probably the network-like structure of DES plays some protective role against thermal stress.

Overall, this report is a part of our ongoing effort to achieve a holistic physical insight into why proteins remain stable and active in DES. The significance of water in any biophysical event is nearly beyond dispute. Especially, the biological water that directly interacts with protein is a critical controlling factor. Herein we showed that HSA maintains the associated water structure around it in the hydrated DES. Singularly, the first solvation shell around HSA remains unperturbed. Protein, therefore, feels only an aqueous environment in the presence of DES, although the macroscopic properties of the solvent change significantly. We feel that this result is not expected in the light of current knowledge. Our result is probably the first experimental proof that protein remains stable and active in DES by keeping its associated water structure intact. We understand that a huge effort is necessary to generalize our claim by taking different DESs and proteins. We also acknowledge that a comparison of complete solvation dynamics, thermodynamic stability parameters, and enzymatic activity are essential. Our future works are aimed at this.

CRediT authorship contribution statement

TK- Conceptualization, methodology, investigation, formal analysis, data curation, writing original draft, review & editing, visualization.

ND- Conceptualization, writing original draft, review & editing, visualization, creative discussion.

KN- help in acquiring solvation data, discussion.

SB- TA data acquisition.

PS- Conceptualization, review & editing, visualization, discussion, supervision, funding acquisition.

Declaration of competing interest

Authors declare no conflict of interest.

Acknowledgments

TK thanks the Prime Minister Research Fellowship, Government of India for graduate studies. ND, KN, and SB gratefully acknowledge Council of Scientific & Industrial Research (CSIR), India, Indian Institute of Technology Kanpur, and University Grants Commission (UGC), India, respectively, for providing graduate fellowship. Authors thank the Department of Chemical Engineering, IIT Bombay, India for Karl Fischer titration. Authors also thank Mr. Abhineet Verma and Dr. Satyen Saha of Department of Chemistry, Benaras Hindu University, India for measuring the viscosities of the solvents. PS thanks the Indian Institute of Technology Kanpur for infrastructure and Poonam and Prabhu Goel Chair position of IIT Kanpur for support. This work is financially supported by the Science and Engineering Research Board, Government of India (Grant No. CRG/2022/002324).

Appendix A. Supplementary data

Confirmation of tagging, fluorescence correlation spectroscopy: setup and data fitting, time-resolved emission spectra, steady-state emission spectra, fluorescence intensity autocorrelation curve, time-resolved stimulated emission spectra, melting curve of CPM tagged HSA. Supplementary data to this article can be found online at doi: https://doi.org/10.1016/j.ijbiomac.2023.127100.

References

[1] B. Hauer, Embracing nature's catalysts: a viewpoint on the future of biocatalysis, ACS Catal. 10 (2020) 8418–8427, https://doi.org/10.1021/acscatal.0c01708.
[2] A. Madhavan, R. Sindhu, P. Binod, R.K. Sukumaran, A. Pandey, Strategies for design of improved biocatalysts for industrial applications, Bioresour. Technol. 245 (2017) 1304–1313, https://doi.org/10.1016/j.biortech.2017.05.031.
[3] A.S. Bommarius, M.F. Paye, Stabilizing biocatalysts, Chem. Soc. Rev. 42 (2013) 6534–6565, https://doi.org/10.1039/c3cs60137d.
[4] P.K. Robinson, Enzymes: principles and biotechnological applications, Essays Biochem. 59 (2015) 1–41, https://doi.org/10.1042/BSE0590001.
[5] K. Chen, F.H. Arnold, Tuning the activity of an enzyme for unusual environments: sequential random mutagenesis of subtilisin E for catalysis in dimethylformamide, Proc. Natl. Acad. Sci. U. S. A. 90 (1993) 5618–5622.
[6] F.H. Arnold, Protein engineering for unusual environments, Curr. Opin. Biotechnol. 4 (1993) 450–455.
[7] R. Fasan, M.M. Chen, N.C. Crook, F.H. Arnold, Engineered alkane-hydroxylating cytochrome P450BM3 exhibiting nativelike catalytic properties, Angew. Chem. Int. Ed. 46 (2007) 8414–8418, https://doi.org/10.1002/anie.200702616.
[8] A. Zaks, A.M. Klibanov, Enzymatic catalysis in organic media at 100°C, Science 224 (1984) (1979) 1249–1251, https://doi.org/10.1126/science.6729453.
[9] A.M. Klibanov, Improving enzymes by using them in organic solvents, Nature. 409 (2001) 241–246. www.nature.com.
[10] M. Panić, M. Cvjetko Bubalo, I. Radojčić Redovniković, Designing a biocatalytic process involving deep eutectic solvents, J. Chem. Technol. Biotechnol. 96 (2021) 14–30, https://doi.org/10.1002/jctb.6545.
[11] F. van Rantwijk, R.A. Sheldon, Biocatalysis in ionic liquids, Chem. Rev. 107 (2007) 2757–2785, https://doi.org/10.1021/cr050946x.
[12] V. Stepankova, S. Bidmanova, T. Koudelakova, Z. Prokop, R. Chaloupkova, J. Damborsky, Strategies for stabilization of enzymes in organic solvents, ACS Catal. 3 (2013) 2823–2836, https://doi.org/10.1021/cs400684x.
[13] D.K. Das, A.K. Das, A.K. Mandal, T. Mondal, K. Bhattacharyya, Effect of an ionic liquid on the unfolding of human serum albumin: a fluorescence correlation spectroscopy study, ChemPhysChem. 13 (2012) 1949–1955, https://doi.org/10.1002/cphc.201100421.
[14] D.C. Murador, L.M. de Souza Mesquita, N. Vannuchi, A.R.C. Braga, V.V. de Rosso, Bioavailability and biological effects of bioactive compounds extracted with natural deep eutectic solvents and ionic liquids: advantages over conventional organic solvents, Curr. Opin. Food Sci. 26 (2019) 25–34, https://doi.org/10.1016/j.cofs.2019.03.002.
[15] R.A. Sheldon, Biocatalysis in ionic liquids: state-of-the-union, Green Chem. 23 (2021) 8406–8427, https://doi.org/10.1039/d1gc03145g.
[16] S.H. Schöfer, N. Kaftzik, P. Wasserscheid, U. Kragl, Enzyme catalysis in ionic liquids: lipase catalysed kinetic resolution of 1-phenylethanol with improved enantioselectivity, Chem. Commun. (2001) 425–426, https://doi.org/10.1039/b009389k.
[17] J.E. Bara, A. Finotello, J.W. Magee, S. Qian, K.E. O'Harra, G.P. Dennis, R. D. Noble, 110th anniversary: properties of imidazolium-based ionic liquids bearing both benzylic and n-alkyl substituents, Ind. Eng. Chem. Res. 58 (2019) 17956–17964, https://doi.org/10.1021/acs.iecr.9b03159.
[18] Y. Liu, X. Chen, S. Men, P. Licence, F. Xi, Z. Ren, W. Zhu, The impact of cation acidity and alkyl substituents on the cation-anion interactions of 1-alkyl-2,3-dimethylimidazolium ionic liquids, Phys. Chem. Chem. Phys. 21 (2019) 11058–11065, https://doi.org/10.1039/c9cp01381d.
[19] J. Płotka-Wasylka, M. de la Guardia, V. Andruch, M. Vilková, Deep eutectic solvents vs ionic liquids: Similarities and differences, Microchem. J. 159 (2020), https://doi.org/10.1016/j.microc.2020.105539.
[20] E.L. Smith, A.P. Abbott, K.S. Ryder, Deep eutectic solvents (DESs) and their applications, Chem. Rev. 114 (2014) 11060–11082, https://doi.org/10.1021/cr300162p.
[21] P. Domínguez de María, Z. Maugeri, Ionic liquids in biotransformations: from proof-of-concept to emerging deep-eutectic-solvents, Curr. Opin. Chem. Biol. 15 (2011) 220–225, https://doi.org/10.1016/j.cbpa.2010.11.008.
[22] F.S. Mjalli, O.U. Ahmed, Physical properties and intermolecular interaction of eutectic solvents binary mixtures: reline and ethaline, Asia Pac. J. Chem. Eng. 11 (2016) 549–557, https://doi.org/10.1002/apj.1978.
[23] W. Guo, Y. Hou, S. Ren, S. Tian, W. Wu, Formation of deep eutectic solvents by phenols and choline chloride and their physical properties, J. Chem. Eng. Data 58 (2013) 866–872, https://doi.org/10.1021/je300997v.
[24] N. Yadav, P. Venkatesu, Current understanding and insights towards protein stabilization and activation in deep eutectic solvents as sustainable solvent media, Phys. Chem. Chem. Phys. 24 (2022) 13474–13509, https://doi.org/10.1039/D2CP00084A.

[25] M. Pätzold, S. Siebenhaller, S. Kara, A. Liese, C. Syldatk, D. Holtmann, Deep eutectic solvents as efficient solvents in biocatalysis, Trends Biotechnol. 37 (2019) 943–959, https://doi.org/10.1016/j.tibtech.2019.03.007.
[26] J.A. Kist, H. Zhao, K.R. Mitchell-Koch, G.A. Baker, The study and application of biomolecules in deep eutectic solvents, J. Mater. Chem. B 9 (2021) 536–566, https://doi.org/10.1039/d0tb01656j.
[27] J.S. Almeida, E.V. Capela, A.M. Loureiro, A.P.M. Tavares, M.G. Freire, An overview on the recent advances in alternative solvents as stabilizers of proteins and enzymes, ChemEngineering 6 (2022), https://doi.org/10.3390/chemengineering6040051.
[28] S.H. Kim, S. Park, H. Yu, J.H. Kim, H.J. Kim, Y.H. Yang, Y.H. Kim, K.J. Kim, E. Kan, S.H. Lee, Effect of deep eutectic solvent mixtures on lipase activity and stability, J. Mol. Catal. B Enzym. 128 (2016) 65–72, https://doi.org/10.1016/j.molcatb.2016.03.012.
[29] I. Juneidi, M. Hayyan, M.A. Hashim, A. Hayyan, Pure and aqueous deep eutectic solvents for a lipase-catalysed hydrolysis reaction, Biochem. Eng. J. 117 (2017) 129–138, https://doi.org/10.1016/j.bej.2016.10.003.
[30] B. Nian, C. Cao, Y. Liu, How Candida antarctica lipase B can be activated in natural deep eutectic solvents: experimental and molecular dynamics studies, J. Chem. Technol. Biotechnol. 95 (2020) 86–93, https://doi.org/10.1002/jctb.6209.
[31] A. Sanchez-Fernandez, M. Basic, J. Xiang, S. Prevost, A.J. Jackson, C. Dicko, Hydration in deep eutectic solvents induces non-monotonic changes in the conformation and stability of proteins, J. Am. Chem. Soc. 144 (2022) 23657–23667, https://doi.org/10.1021/jacs.2c11190.
[32] A. Sanchez-Fernandez, K.J. Edler, T. Arnold, D. Alba Venero, A.J. Jackson, Protein conformation in pure and hydrated deep eutectic solvents, Phys. Chem. Chem. Phys. 19 (2017) 8667–8670, https://doi.org/10.1039/c7cp00459a.
[33] A. Sanchez-Fernandez, A.J. Jackson, Proteins in deep eutectic solvents: Structure, dynamics and interactions with the solvent, in: Adv Bot Res, Academic Press Inc., 2021, pp. 69–94, https://doi.org/10.1016/bs.abr.2020.09.003.
[34] C. Ma, A. Laaksonen, C. Liu, X. Lu, X. Ji, The peculiar effect of water on ionic liquids and deep eutectic solvents, Chem. Soc. Rev. 47 (2018) 8685–8720, https://doi.org/10.1039/c8cs00325d.
[35] Y. Dai, G.J. Witkamp, R. Verpoorte, Y.H. Choi, Tailoring properties of natural deep eutectic solvents with water to facilitate their applications, Food Chem. 187 (2015) 14–19, https://doi.org/10.1016/j.foodchem.2015.03.123.
[36] R. Esquembre, J.M. Sanz, J.G. Wall, F. Del Monte, C.R. Mateo, M.L. Ferrer, Thermal unfolding and refolding of lysozyme in deep eutectic solvents and their aqueous dilutions, Phys. Chem. Chem. Phys. 15 (2013) 11248–11256, https://doi.org/10.1039/c3cp44299c.
[37] R. Xin, S. Qi, C. Zeng, F.I. Khan, B. Yang, Y. Wang, A functional natural deep eutectic solvent based on trehalose: structural and physicochemical properties, Food Chem. 217 (2017) 560–567, https://doi.org/10.1016/j.foodchem.2016.09.012.
[38] F. Niknaddaf, S.S. Shahangian, A. Heydari, S. Hosseinkhani, R.H. Sajedi, Deep eutectic solvents as a new generation of chemical chaperones, ChemistrySelect. 3 (2018) 10603–10607, https://doi.org/10.1002/slct.201802235.
[39] J.T. Gorke, F. Srienc, R.J. Kazlauskas, Deep eutectic solvents for Candida antarctica lipase B-catalyzed reactions, in: ACS Symposium Series, 2010, pp. 169–180, https://doi.org/10.1021/bk-2010-1038.ch014.
[40] E. Durand, J. Lecomte, B. Baréa, E. Dubreucq, R. Lortie, P. Villeneuve, Evaluation of deep eutectic solvent-water binary mixtures for lipase-catalyzed lipophilization of phenolic acids, Green Chem. 15 (2013) 2275–2282, https://doi.org/10.1039/c3gc40899j.
[41] E. Durand, J. Lecomte, B. Baréa, P. Villeneuve, Towards a better understanding of how to improve lipase-catalyzed reactions using deep eutectic solvents based on choline chloride, Eur. J. Lipid Sci. Technol. 116 (2014) 16–23, https://doi.org/10.1002/ejlt.201300246.
[42] Z.L. Huang, B.P. Wu, Q. Wen, T.X. Yang, Z. Yang, Deep eutectic solvents can be viable enzyme activators and stabilizers, J. Chem. Technol. Biotechnol. 89 (2014) 1975–1981, https://doi.org/10.1002/jctb.4285.
[43] M. Cvjetko Bubalo, A. Jurinjak Tušek, M. Vinković, K. Radošević, V. Gaurina Srček, I. Radojčić Redovniković, Cholinium-based deep eutectic solvents and ionic liquids for lipase-catalyzed synthesis of butyl acetate, J. Mol. Catal. B Enzym. 122 (2015) 188–198, https://doi.org/10.1016/j.molcatb.2015.09.005.
[44] N. Yadav, K. Bhakuni, M. Bisht, I. Bahadur, P. Venkatesu, Expanding the potential role of deep eutectic solvents toward facilitating the structural and thermal stability of α-chymotrypsin, ACS Sustain. Chem. Eng. 8 (2020) 10151–10160, https://doi.org/10.1021/acssuschemeng.0c02213.
[45] N. Das, T. Khan, N. Subba, P. Sen, Correlating Bromelain's activity with its structure and active-site dynamics and the medium's physical properties in a hydrated deep eutectic solvent, Phys. Chem. Chem. Phys. 23 (2021) 9337–9346, https://doi.org/10.1039/d1cp00046b.
[46] H. Sun, R. Xin, D. Qu, F. Yao, Mechanism of deep eutectic solvents enhancing catalytic function of cytochrome P450 enzymes in biosynthesis and organic synthesis, J. Biotechnol. 323 (2020) 264–273, https://doi.org/10.1016/j.jbiotec.2020.07.004.
[47] S.S. Hossain, S. Paul, A. Samanta, Structural stability and conformational dynamics of cytochrome c in hydrated deep eutectic solvents, J. Phys. Chem. B 125 (2021) 5757–5765, https://doi.org/10.1021/acs.jpcb.1c01975.
[48] K. Bhattacharyya, Nature of biological water: a femtosecond study, Chem. Commun. (2008) 2848–2857, https://doi.org/10.1039/b800278a.
[49] B. Bagchi, Water dynamics in the hydration layer around proteins and micelles, Chem. Rev. 105 (2005) 3197–3219, https://doi.org/10.1021/cr020661+.
[50] N. Das, E. Tarif, A. Dutta, P. Sen, Associated water dynamics might be a key factor affecting protein stability in the crowded milieu, J. Phys. Chem. B 127 (2023) 3151–3163, https://doi.org/10.1021/acs.jpcb.2c09043.
[51] S. Mondal, S. Mukherjee, B. Bagchi, Protein hydration dynamics: much ado about nothing? J. Phys. Chem. Lett. 8 (2017) 4878–4882, https://doi.org/10.1021/acs.jpclett.7b02324.
[52] Y. Qin, L. Wang, D. Zhong, Dynamics and mechanism of ultrafast water- protein interactions, Proc. Natl. Acad. Sci. U. S. A. 113 (2016) 8424–8429, https://doi.org/10.1073/pnas.1602916113.
[53] S.K. Pal, J. Peon, B. Bagchi, A.H. Zewail, Biological water: femtosecond dynamics of macromolecular hydration, J. Phys. Chem. B 106 (2002) 12376–12395, https://doi.org/10.1021/jp0213506.
[54] M.C. Bellissent-Funel, A. Hassanali, M. Havenith, R. Henchman, P. Pohl, F. Sterpone, D. Van Der Spoel, Y. Xu, A.E. Garcia, Water determines the structure and dynamics of proteins, Chem. Rev. 116 (2016) 7673–7697, https://doi.org/10.1021/acs.chemrev.5b00664.
[55] S.K. Pal, J. Peon, A.H. Zewail, Ultrafast surface hydration dynamics and expression of protein functionality: α-chymotrypsin, Proc. Natl. Acad. Sci. U. S. A. 99 (2002) 15297–15302, https://doi.org/10.1073/pnas.242600399.
[56] P.K. Verma, S. Rakshit, R.K. Mitra, S.K. Pal, Role of hydration on the functionality of a proteolytic enzyme α-chymotrypsin under crowded environment, Biochimie. 93 (2011) 1424–1433, https://doi.org/10.1016/j.biochi.2011.04.017.
[57] P. Ball, Water as an active constituent in cell biology, Chem. Rev. 108 (2008) 74–108, https://doi.org/10.1021/cr068037a.
[58] N. Shukla, E. Pomarico, L. Chen, M. Chergui, C.M. Othon, Retardation of bulk water dynamics by disaccharide osmolytes, J. Phys. Chem. B 120 (2016) 9477–9483, https://doi.org/10.1021/acs.jpcb.6b07751.
[59] F. Guo, J.M. Friedman, Osmolyte-induced perturbations of hydrogen bonding between hydration layer waters: correlation with protein conformational changes, J. Phys. Chem. B 113 (2009) 16632–16642, https://doi.org/10.1021/jp9072284.
[60] M. Hishida, R. Anjum, T. Anada, D. Murakami, M. Tanaka, Effect of osmolytes on water mobility correlates with their stabilizing effect on proteins, J. Phys. Chem. B 126 (2022) 2466–2475, https://doi.org/10.1021/acs.jpcb.1c10634.
[61] P. Trodler, J. Pleiss, Modeling structure and flexibility of Candida antarctica lipase B in organic solvents, BMC Struct. Biol. 8 (2008), https://doi.org/10.1186/1472-6807-8-9.
[62] M. Shehata, A. Unlu, U. Sezerman, E. Timucin, Lipase and water in a deep eutectic solvent: molecular dynamics and experimental studies of the effects of water-in-deep eutectic solvents on lipase stability, J. Phys. Chem. B 124 (2020) 8801–8810, https://doi.org/10.1021/acs.jpcb.0c07041.
[63] R. Wedberg, J. Abildskov, G.H. Peters, Protein dynamics in organic media at varying water activity studied by molecular dynamics simulation, J. Phys. Chem. B 116 (2012) 2575–2585, https://doi.org/10.1021/jp211054u.
[64] J.P. Bittner, N. Zhang, L. Huang, P. Domínguez De María, S. Jakobtorweihen, S. Kara, Impact of deep eutectic solvents (DESs) and individual des components on alcohol dehydrogenase catalysis: connecting experimental data and molecular dynamics simulations, Green Chem. 24 (2022) 1120–1131, https://doi.org/10.1039/d1gc04059f.
[65] H. Monhemi, M.R. Housaindokht, A.A. Moosavi-Movahedi, M.R. Bozorgmehr, How a protein can remain stable in a solvent with high content of urea: Insights from molecular dynamics simulation of Candida antarctica lipase B in urea: Choline chloride deep eutectic solvent, in: Physical Chemistry Chemical Physics, Royal Society of Chemistry, 2014, pp. 14882–14893, https://doi.org/10.1039/c4cp00503a.
[66] V.P. Denisov, B.H. Jonsson, B. Halle, Hydration of denatured and molten globule proteins, Nat. Struct. Biol. 6 (1999) 253–260, https://doi.org/10.1038/6692.
[67] G. Otting, E. Liepinsh, K. Wüthrich, Protein hydration in aqueous solution, Science 254 (1991) (1979) 974–980, https://doi.org/10.1126/science.1948083.
[68] N. Nandi, K. Bhattacharyya, B. Bagchi, Dielectric relaxation and solvation dynamics of water in complex chemical and biological systems, Chem. Rev. 100 (2000) 2013–2045, https://doi.org/10.1021/cr980127v.
[69] D. Russo, R.K. Murarka, J.R.D. Copley, T. Head-Gordon, Molecular view of water dynamics near model peptides, J. Phys. Chem. B 109 (2005) 12966–12975, https://doi.org/10.1021/jp051137k.
[70] W. Qiu, L. Zhang, O. Okobiah, Y. Yang, L. Wang, D. Zhong, A.H. Zewail, Ultrafast solvation dynamics of human serum albumin: correlations with conformational transitions and site-selected recognition, J. Phys. Chem. B 110 (2006) 10540–10549, https://doi.org/10.1021/jp055989w.
[71] H. Rastogi, P.K. Chowdhury, Correlating the local and global dynamics of an enzyme in the crowded milieu, J. Phys. Chem. B 126 (2022) 3208–3223, https://doi.org/10.1021/acs.jpcb.1c09759.
[72] S.K. Pal, D. Mandai, D. Sukul, S. Sen, K. Bhattacharyya, Solvation dynamics of DCM in human serum albumin, J. Phys. Chem. B 105 (2001) 1438–1441, https://doi.org/10.1021/jp002368o.
[73] P. Houston, N. Macro, M. Kang, L. Chen, J. Yang, L. Wang, Z. Wu, D. Zhong, Ultrafast dynamics of water-protein coupled motions around the surface of eye crystallin, J. Am. Chem. Soc. 142 (2020) 3997–4007, https://doi.org/10.1021/jacs.9b13506.
[74] L. Zhang, L. Wang, Y.-T. Kao, W. Qiu, Y. Yang, O. Okobiah, D. Zhong, Mapping Hydration Dynamics Around a Protein Surface 104, 2007, pp. 18461–18466.
[75] M. Maroncelli, G.R. Fleming, Picosecond solvation dynamics of coumarin 153: the importance of molecular aspects of solvation, J. Chem. Phys. 86 (1987) 6221–6239, https://doi.org/10.1063/1.452460.

[76] N. Das, P. Sen, Structural, functional, and dynamical responses of a protein in a restricted environment imposed by macromolecular crowding, Biochemistry. 57 (2018) 6078–6089, https://doi.org/10.1021/acs.biochem.8b00599.
[77] N. Das, S. Yadav, K.S. Negi, E. Tarif, P. Sen, Does microsecond active-site dynamics primarily control proteolytic activity of bromelain? Clues from single molecular level study with a denaturant, a stabilizer and a macromolecular crowder, BBA Advances. 2 (2022) 100041, https://doi.org/10.1016/j.bbadva.2022.100041.
[78] N. Das, P. Sen, Macromolecular crowding: how shape and interaction affect the structure, function, conformational dynamics and relative domain movement of a multi-domain protein, Phys. Chem. Chem. Phys. 24 (2022) 14242–14256, https://doi.org/10.1039/D1CP04842B.
[79] J.M. Yon, D. Perahia, C. Ghélis, Conformational dynamics and enzyme activity, Biochimie. 80 (1998) 33–42, https://doi.org/10.1016/S0300-9084(98)80054-0.
[80] J. Guo, H.X. Zhou, Protein allostery and conformational dynamics, Chem. Rev. 116 (2016) 6503–6515, https://doi.org/10.1021/acs.chemrev.5b00590.
[81] K.R. Torgeson, M.W. Clarkson, D. Granata, K. Lindorff-Larsen, R. Page, W. Peti, Conserved conformational dynamics determine enzyme activity, Sci. Adv. 8 (2022), eabo5546, https://doi.org/10.1126/sciadv.abo5546.
[82] A. Nandy, S. Chakraborty, S. Nandi, K. Bhattacharyya, S. Mukherjee, Structure, activity, and dynamics of human serum albumin in a crowded Pluronic F127 hydrogel, J. Phys. Chem. B 123 (2019) 3397–3408, https://doi.org/10.1021/acs.jpcb.9b00219.
[83] S. Shil, N. Das, B. Sengupta, P. Sen, Sucrose-induced stabilization of domain-II and overall human serum albumin against chemical and thermal denaturation, ACS Omega. 3 (2018) 16633–16642, https://doi.org/10.1021/acsomega.8b01832.
[84] B. Sengupta, N. Das, P. Sen, Elucidation of μs dynamics of domain-III of human serum albumin during the chemical and thermal unfolding: a fluorescence correlation spectroscopic investigation, Biophys. Chem. 221 (2017) 17–25, https://doi.org/10.1016/j.bpc.2016.11.006.
[85] R. Yadav, B. Sengupta, P. Sen, Conformational fluctuation dynamics of domain i of human serum albumin in the course of chemically and thermally induced unfolding using fluorescence correlation spectroscopy, J. Phys. Chem. B 118 (2014) 5428–5438, https://doi.org/10.1021/jp502762t.
[86] B. Sengupta, A. Acharyya, P. Sen, Elucidation of the local dynamics of domain-III of human serum albumin over the ps–μs time regime using a new fluorescent label, Phys. Chem. Chem. Phys. 18 (2016) 28548–28555, https://doi.org/10.1039/C6CP05743H.
[87] N. Das, S. Sahu, T. Khan, P. Sen, Site-specific heterogeneity of multi-domain human serum albumin and its origin: a red edge excitation shift study, Photochem. Photobiol. 99 (2023) 538–546, https://doi.org/10.1111/php.13712.
[88] S. Curry, H. Mandelkow, P. Brick, N. Franks, Crystal structure of human serum albumin complexed with fatty acid reveals an asymmetric distribution of binding sites, Nat. Struct. Biol. 5:9 (5) (1998) 827–835, https://doi.org/10.1038/1869.
[89] J.T. Gorke, F. Srienc, R.J. Kazlauskas, Hydrolase-catalyzed biotransformations in deep eutectic solvents, Chem. Commun. (2008) 1235–1237, https://doi.org/10.1039/b716317g.
[90] M.L. Toledo, M.M. Pereira, M.G. Freire, J.P.A. Silva, J.A.P. Coutinho, A.P. M. Tavares, Laccase activation in deep eutectic solvents, ACS Sustain. Chem. Eng. 7 (2019) 11806–11814, https://doi.org/10.1021/acssuschemeng.9b02179.
[91] J. Cao, E. Su, Hydrophobic deep eutectic solvents: the new generation of green solvents for diversified and colorful applications in green chemistry, J. Clean. Prod. 314 (2021), https://doi.org/10.1016/j.jclepro.2021.127965.
[92] D.J.G.P. Van Osch, C.H.J.T. Dietz, S.E.E. Warrag, M.C. Kroon, The curious case of hydrophobic deep eutectic solvents: a story on the discovery, design, and applications, ACS Sustain. Chem. Eng. 8 (2020) 10591–10612, https://doi.org/10.1021/acssuschemeng.0c00559.
[93] D.J.G.P. Van Osch, C.H.J.T. Dietz, J. Van Spronsen, M.C. Kroon, F. Gallucci, M. Van Sint Annaland, R. Tuinier, A search for natural hydrophobic deep eutectic solvents based on natural components, ACS Sustain. Chem. Eng. 7 (2019) 2933–2942, https://doi.org/10.1021/acssuschemeng.8b03520.
[94] N. Subba, K. Polok, P. Piatkowski, B. Ratajska-Gadomska, R. Biswas, W. Gadomski, P. Sen, Temperature-dependent ultrafast solvation response and solute diffusion in acetamide-urea deep eutectic solvent, J. Phys. Chem. B 123 (2019) 9212–9221, https://doi.org/10.1021/ACS.JPCB.9B07794.
[95] K. Mukherjee, S. Das, E. Tarif, A. Barman, R. Biswas, Dielectric relaxation in acetamide + urea deep eutectics and neat molten urea: origin of time scales via temperature dependent measurements and computer simulations, J. Chem. Phys. 149 (2018) 124501, https://doi.org/10.1063/1.5040071.
[96] S. Suriyanarayanan, G.D. Olsson, S. Kathiravan, N. Ndizeye, I.A. Nicholls, Non-ionic deep eutectic liquids: Acetamide–urea derived room temperature solvents, Int. J. Mol. Sci. 20 (2019), https://doi.org/10.3390/ijms20122857.
[97] N. Subba, P. Sahu, N. Das, P. Sen, Rational design, preparation and characterization of a ternary non-ionic room-temperature deep eutectic solvent derived from urea, acetamide, and sorbitol, J. Chem. Sci. 133 (2021) 25, https://doi.org/10.1007/s12039-020-01866-2.
[98] T. Khan, E. Tarif, Y. Awano, L.S. Lozada, N. Das, K. Tominaga, P. Sen, Multiple evidences for molecular level heterogeneity in a non-ionic biocatalytic deep eutectic solvent, J. Mol. Liq. 389 (2023) 122882, https://doi.org/10.1016/j.molliq.2023.122882.
[99] G. Bohm, R. Muhr, R. Jaenicke, Quantitative analysis of protein far UV circular dichroism spectra by neural networks, Protein Eng. 5 (1992) 191–195. https://academic.oup.com/peds/article/5/3/191/1535269.
[100] N. Das, P. Sen, Shape-dependent macromolecular crowding on the thermodynamics and microsecond conformational dynamics of protein unfolding revealed at the single-molecule level, J. Phys. Chem. B 124 (2020) 5858–5871, https://doi.org/10.1021/acs.jpcb.0c03897.
[101] N. Subba, N. Das, P. Sen, Partial viscosity decoupling of solute solvation, rotation, and translation dynamics in Lauric acid/menthol deep eutectic solvent: modulation of dynamic heterogeneity with length scale, J. Phys. Chem. B 124 (2020) 6875–6884, https://doi.org/10.1021/acs.jpcb.0c04379.
[102] E. Tarif, N. Das, P. Sen, Does viscosity decoupling guarantee dynamic heterogeneity? A clue through an excitation and emission wavelength-dependent time-resolved fluorescence anisotropy study, J. Phys. Chem. B (2023), https://doi.org/10.1021/acs.jpcb.3c00334.
[103] J.R. Lakowicz, Principles of Fluorescence Spectroscopy, Springer, 2006, https://doi.org/10.1007/978-0-387-46312-4.
[104] S. Kumar, J. Peon, A.H. Zewail, Biological water at the protein surface: dynamical solvation probed directly with femtosecond resolution, Proc. Natl. Acad. Sci. U. S. A. 99 (2002) 1763–1768. www.pnas.orgcgidoi10.1073pnas.042697899.
[105] M.L. Horng, J.A. Gardecki, A. Papazyan, M. Maroncelli, Subpicosecond measurements of polar solvation dynamics: Coumarin 153 revisited, J. Phys. Chem. 99 (1995) 17311–17337, https://doi.org/10.1021/J100048A004.
[106] P. Mukherjee, A. Das, A. Sengupta, P. Sen, Bimolecular photoinduced electron transfer in static quenching regime: illustration of Marcus inversion in micelle, J. Phys. Chem. B 121 (2017) 1610–1622, https://doi.org/10.1021/acs.jpcb.6b11206.
[107] R. Berera, R. van Grondelle, J.T.M. Kennis, Ultrafast transient absorption spectroscopy: principles and application to photosynthetic systems, Photosynth. Res. 101 (2009) 105–118, https://doi.org/10.1007/s11120-009-9454-y.
[108] O.S. Hammond, D.T. Bowron, K.J. Edler, The effect of water upon deep eutectic solvent nanostructure: an unusual transition from ionic mixture to aqueous solution, Angew. Chem. 129 (2017) 9914–9917, https://doi.org/10.1002/ange.201702486.
[109] T. El Achkar, S. Fourmentin, H. Greige-Gerges, Deep eutectic solvents: An overview on their interactions with water and biochemical compounds, J. Mol. Liq. 288 (2019), https://doi.org/10.1016/j.molliq.2019.111028.
[110] Y. Dai, G.J. Witkamp, R. Verpoorte, Y.H. Choi, Tailoring properties of natural deep eutectic solvents with water to facilitate their applications, Food Chem. 187 (2015) 14–19, https://doi.org/10.1016/j.foodchem.2015.03.123.
[111] C. D'Agostino, L.F. Gladden, M.D. Mantle, A.P. Abbott, E.I. Ahmed, A.Y.M. Al-Murshedi, R.C. Harris, Molecular and ionic diffusion in aqueous-deep eutectic solvent mixtures: probing inter-molecular interactions using PFG NMR, Phys. Chem. Chem. Phys. 17 (2015) 15297–15304, https://doi.org/10.1039/c5cp01493j.
[112] G.C. Dugoni, M.E. Di Pietro, M. Ferro, F. Castiglione, S. Ruellan, T. Moufawad, L. Moura, M.F. Costa Gomes, S. Fourmentin, A. Mele, Effect of water on deep eutectic solvent/β-cyclodextrin systems, ACS Sustain. Chem. Eng. 7 (2019) 7277–7285, https://doi.org/10.1021/acssuschemeng.9b00315.
[113] R. Schiller, The stokes-einstein law by macroscopic arguments, Int. J. Radiat. Appl. Instrum. 37 (1991) 549–550.
[114] N. Das, P. Sen, Dynamic heterogeneity and viscosity decoupling: origin and analytical prediction, Phys. Chem. Chem. Phys. 23 (2021) 15749–15757, https://doi.org/10.1039/d1cp01804c.
[115] N. Das, N. Subba, P. Sen, Viscosity decoupling does not guarantee dynamic heterogeneity: a way out, J. Photochem. Photobiol. A Chem. 436 (2023) 114361, https://doi.org/10.1016/J.JPHOTOCHEM.2022.114361.
[116] S. Mukherjee, S. Mondal, B. Bagchi, Distinguishing dynamical features of water inside protein hydration layer: distribution reveals what is hidden behind the average, J. Chem. Phys. 147 (2017), 024901, https://doi.org/10.1063/1.4990693.
[117] S. Mondal, S. Mukherjee, B. Bagchi, Origin of diverse time scales in the protein hydration layer solvation dynamics: a simulation study, J. Chem. Phys. 147 (2017) 154901, https://doi.org/10.1063/1.4995420.
[118] P.T. Wingfield, Use of protein folding reagents, Curr Protoc Protein Sci 2016 (2016) A.3A.1–A.3A.8, https://doi.org/10.1002/0471140864.psa03as84.
[119] W.T. Heller, Comparison of the thermal denaturing of human serum albumin in the presence of guanidine hydrochloride and 1-butyl-3-methylimidazolium ionic liquids, J. Phys. Chem. B 117 (2013) 2378–2383, https://doi.org/10.1021/jp400079p.
[120] B. Ahmad, M.Z. Ahmed, S.K. Haq, R.H. Khan, Guanidine hydrochloride denaturation of human serum albumin originates by local unfolding of some stable loops in domain III, Biochim. Biophys. Acta, Proteins Proteomics 1750 (2005) 93–102, https://doi.org/10.1016/j.bbapap.2005.04.001.
[121] V. Mohan, B. Sengupta, A. Acharyya, R. Yadav, N. Das, P. Sen, Region-specific double denaturation of human serum albumin: combined effects of temperature and GnHCl on structural and dynamical responses, ACS Omega 3 (2018) 10406–10417, https://doi.org/10.1021/acsomega.8b00967.
[122] A.W. Kahsai, S. Rajagopal, J. Sun, K. Xiao, Monitoring protein conformational changes and dynamics using stable-isotope labeling and mass spectrometry, Nat. Protoc. 9 (2014) 1301–1319, https://doi.org/10.1038/nprot.2014.075.
[123] V.K. Gangupomu, J.R. Wagner, I.H. Park, A. Jain, N. Vaidehi, Mapping conformational dynamics of proteins using torsional dynamics simulations, Biophys. J. 104 (2013) 1999–2008, https://doi.org/10.1016/j.bpj.2013.01.050.
[124] S. Sen Mojumdar, R. Chowdhury, S. Chattoraj, K. Bhattacharyya, Role of ionic liquid on the conformational dynamics in the native, molten globule, and unfolded states of cytochrome C: a fluorescence correlation spectroscopy study, J. Phys. Chem. B 116 (2012) 12189–12198, https://doi.org/10.1021/jp307297s.
[125] S. Barik, A. Mahapatra, N. Preeyanka, M. Sarkar, Assessing the impact of choline chloride and benzyltrimethylammonium chloride-based deep eutectic solvents on the structure and conformational dynamics of bovine serum albumin: a combined

steady-state, time-resolved fluorescence and fluorescence correlation spectroscopic study, Phys. Chem. Chem. Phys. 25 (2023) 20093–20108, https://doi.org/10.1039/d3cp01380d.
[126] S. Haldar, S. Mitra, K. Chattopadhyay, Role of protein stabilizers on the conformation of the unfolded state of cytochrome c and its early folding kinetics: investigation at single molecular resolution, J. Biol. Chem. 285 (2010) 25314–25323, https://doi.org/10.1074/jbc.M110.116673.
[127] N. Das, P. Sen, Size-dependent macromolecular crowding effect on the thermodynamics of protein unfolding revealed at the single molecular level, Int. J. Biol. Macromol. 141 (2019) 843–854, https://doi.org/10.1016/j.ijbiomac.2019.09.029.
[128] S. Sen, H. Kumar, J.B. Udgaonkar, Microsecond dynamics during the binding-induced folding of an intrinsically disordered protein, J. Mol. Biol. 433 (2021), https://doi.org/10.1016/j.jmb.2021.167254.
[129] A. Jha, K. Ishii, J.B. Udgaonkar, T. Tahara, G. Krishnamoorthy, Exploration of the correlation between solvation dynamics and internal dynamics of a protein, Biochemistry. 50 (2011) 397–408, https://doi.org/10.1021/bi101440c.
[130] E. Durand, J. Lecomte, B. Baréa, G. Piombo, E. Dubreucq, P. Villeneuve, Evaluation of deep eutectic solvents as new media for Candida antarctica B lipase catalyzed reactions, Process Biochem. 47 (2012) 2081–2089, https://doi.org/10.1016/j.procbio.2012.07.027.
[131] P. Zhou, X. Wang, B. Yang, F. Hollmann, Y. Wang, Chemoenzymatic epoxidation of alkenes with Candida antarctica lipase B and hydrogen peroxide in deep eutectic solvents, RSC Adv. 7 (2017) 12518–12523, https://doi.org/10.1039/c7ra00805h.
[132] C.X. Zeng, S.J. Qi, R.P. Xin, B. Yang, Y.H. Wang, Synergistic behavior of betaine-urea mixture: formation of deep eutectic solvent, J. Mol. Liq. 219 (2016) 74–78, https://doi.org/10.1016/j.molliq.2016.02.076.
[133] A.E. Delorme, J.M. Andanson, V. Verney, Improving laccase thermostability with aqueous natural deep eutectic solvents, Int. J. Biol. Macromol. 163 (2020) 919–926, https://doi.org/10.1016/j.ijbiomac.2020.07.022.
[134] A.R. Harifi-Mood, R. Ghobadi, A. Divsalar, The effect of deep eutectic solvents on catalytic function and structure of bovine liver catalase, Int. J. Biol. Macromol. 95 (2017) 115–120, https://doi.org/10.1016/j.ijbiomac.2016.11.043.
[135] Q. Zeng, Y. Wang, Y. Huang, X. Ding, J. Chen, K. Xu, Deep eutectic solvents as novel extraction media for protein partitioning, Analyst. 139 (2014) 2565–2573, https://doi.org/10.1039/c3an02235h.
[136] K. Bhakuni, N. Yadav, P. Venkatesu, A novel amalgamation of deep eutectic solvents and crowders as biocompatible solvent media for enhanced structural and thermal stability of bovine serum albumin, Phys. Chem. Chem. Phys. 22 (2020) 24410–24422, https://doi.org/10.1039/d0cp04397d.
[137] N. Yadav, D. Chahar, M. Bisht, P. Venkatesu, Assessing the compatibility of choline-based deep eutectic solvents for the structural stability and activity of cellulase: enzyme sustain at high temperature, Int. J. Biol. Macromol. 249 (2023) 125988, https://doi.org/10.1016/j.ijbiomac.2023.125988.
[138] J.A. Kist, M.T. Henzl, J.L. Bañuelos, G.A. Baker, Calorimetric evaluation of the operational thermal stability of ribonuclease a in hydrated deep eutectic solvents, ACS Sustain. Chem. Eng. 7 (2019) 12682–12687, https://doi.org/10.1021/acssuschemeng.9b02585.

Supplementary Material

for

Understanding the Intricacy of Protein in Hydrated Deep Eutectic Solvent: Solvation Dynamics, Conformational Fluctuation Dynamics and Stability

Tanmoy Khan, Nilimesh Das, Kuldeep Singh Negi, Suman Bhowmik, and Pratik Sen*

Department of Chemistry, Indian Institute of Technology Kanpur, Kanpur – 208 016, UP, India

*Corresponding author, Email: psen@iitk.ac.in

CONTENTS

Section S1: Confirmation, site-selectivity and perturbation related to tagging of fluorophores to HSA:

Human serum albumin contains 35 cysteine residues. However, only Cys-34 in the domain-I is free and all the others are connected through a disulphide bond with another cysteine residue. Thus, a site-specific tagging of CPM or TMR to the Cys-34 residue is very much possible. For this purpose, we have used HSA and dye in 1:1.2 ratio so that there does not remain any extra dye in the reaction mixture. The absorption spectra of CPM do not change upon tagging to HSA. The tagging efficiency was calculated to be 0.88 using absorption spectra of free and tagged dye following standard procedure.[4] CPM itself is a very weakly fluorescent molecule with its emission maximum lies around 480 nm. When tagged to HSA, it shows a blue shift of 17 nm (figure S1). This hints that upon tagging CPM goes inside the protein core.

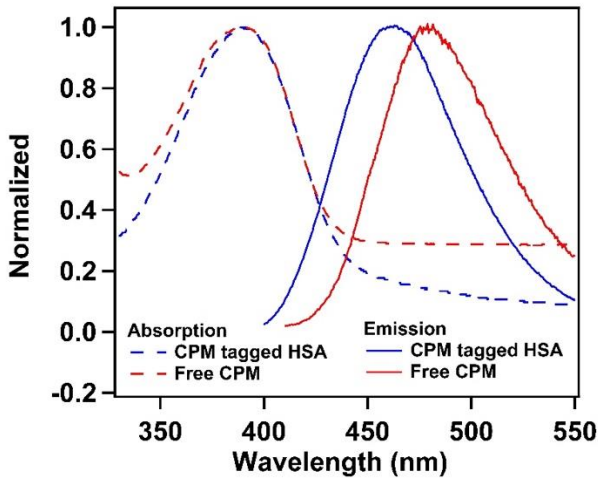

Figure S1. Intensity normalized absorption and emission spectra of free CPM and CPM tagged to HSA.

Due to considerable absorption of the DES itself in the absorption region (~400 nm) of the dye CPM, single molecular measurement with that probe was not possible. Thus, to measure the FCS, we have used a different probe TMR. TMR is not a solvatochromic dye, so after it covalently binds to cys-34 of HSA the absorption and emission spectra of the dye does not change observably. However, this non solvatochromicity of the TMR dye is not a problem for conducting experiments through FCS. Also, the confirmation of TMR tagging has been done using FCS itself (see figure S3). This change of the probe is not going to alter our observations as the probe TMR is attaching with the protein in the exact same place where CPM covalently

bound with. To be sure about that we have measured the thermal stability of unlabelled, HSA attached with TMR, and HSA attached with CPM using CD spectroscopy (Figure S2). All the CD signals and the nature of melting curves are very much similar confirms the same.

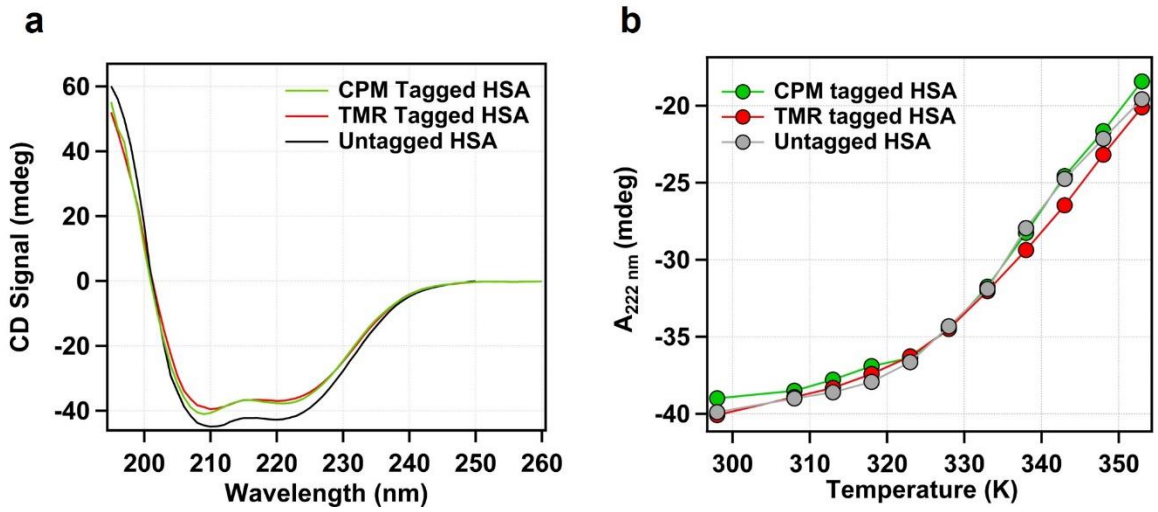

Figure S2. (a) Circular dichroism spectra of untagged, TMR tagged, and CPM tagged HSA at room temperature (298 K), (b) Melting curves of untagged, TMR tagged, and CPM tagged HSA

Table S1. Secondary structural parameters from CD spectra of untagged HSA, TMR tagged HSA and CPM tagged HSA at room temperature (calculated using CDNN software[5]).

	%- of secondary structural contents			
	α- helicity	β- sheet	β- turn	Random coil
Untagged HSA	67.1	5.7	12.8	14.4
TMR tagged HSA	65.5	5.4	13.0	16.1
CPM tagged HSA	66.8	6.0	12.5	14.7

Now we measured the diffusion time of free TMR dye and TMR tagged HSA and the diffusion time come as 45μs and 228 μs respectively. (Figure S3) This increments in the diffusion times while attaching with the protein also confirms the attachment of the probe with the protein under investigation. A similar FCS experiment (as that of free TMR and TMR tagged HSA) with free CPM and CPM tagged to HSA suggests the tagging, and we have already proved that in our previous publications.[6]

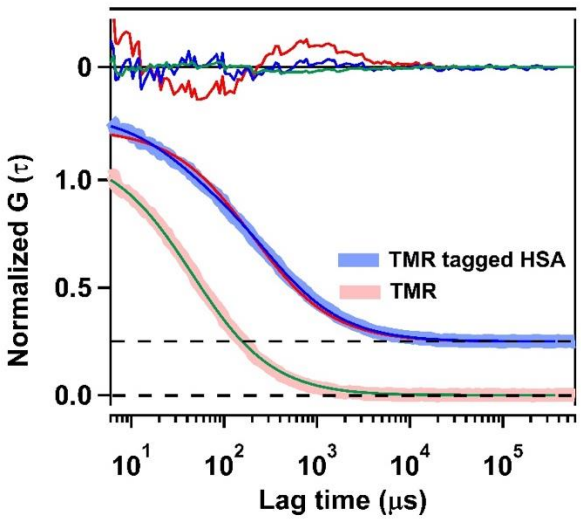

Figure S3. Fluorescence intensity autocorrelation curve of free TMR, and TMR tagged to HSA in phosphate buffer. The autocorrelation function of TMR fits well with equation 3. The fitting lines and the residuals are shown in the figure. The autocorrelations of TMR tagged to HSA cannot be fitted with equation 3 satisfactorily but extra relaxation term is required and can be fitted by equation 4 (see the fitting lines and residual). Autocorrelation trace of TMR-HSA were fitted from 5 μs due to known inherent photo physics of rhodamine dye in 1 μs timescale.

The site-specificity might also be proved from FRET experiment. As discussed in the main text, Trp-CPM forms a very good FRET pair that can give information about the domain-I-domain-II distance of HSA. The distance between CPM attached to Cys-34 of domain-I of HSA and Trp-214 of domain-II of HSA is calculated to be 25 Å. The value matches well with the value from crystal structure.

Section S2: Fluorescence Correlation Spectroscopy (FCS): set up and data fitting

FCS experiments were done with a home-built FCS set-up. An inverted confocal microscope (Olympus IX-71, Japan) with a 60X, 1.2 NA water immersion objective (UplanSApo, Olympus, Japan) along with an excitation source of 532 nm laser source (MGL-III-532-5 mW, CNI, China) was used to create a confocal volume. Other components of the system were a multimode fiber patch chord of 25 μm diameter (M67L01 25 nm 0.10NA, ThorLabs, USA), dichroic mirror (ZT532rdc, Chroma Tech. Corp., USA), emission filter (605/70m, Chroma Tech. Corp., USA), a photon counting module (SPCM-AQRH-13-FC, Excelitas Tech. Inc., Canada), and a correlator card (Flex99OEM-12/E, Correlator.com, USA). The sample was kept on a coverslip (Blue Star, Polar Industrial Corporation) on the sample platform. The focal point was set at 40 μm above the upper surface of the cover slip. The power was optimized to have the best count but no photobleaching. The emitted photons were directed toward the detector through the fiber patch chord. The detected photons were received and autocorrelated by the correlator card and displayed on the LabVIEW platform on a computer.

Autocorrelation function G(τ) that arises because of the temporal fluctuation of the fluorescence intensity can be described as,[1,2]

$$G(\tau) = \frac{\langle \delta F(t) \delta F(t+\tau) \rangle}{\langle F(t) \rangle^2} \qquad \text{(equation 1)}$$

Autocorrelation is the self-similarity of fluorescence intensity at different times. $\langle F(t) \rangle$ is the average fluorescence intensity, and $\delta F(\tau)$ and $\delta F(t+\tau)$ are the quantity of fluctuation in intensity around the mean value at time t and $(t+\tau)$;

$$\delta F(t+\tau) = F(t+\tau) - \langle F(t) \rangle \qquad \text{(equation 2)}$$

For a single-component system, the diffusion time (τ_D) can be obtained by fitting the autocorrelation function G(τ) using the following equation.[1,2]

$$G(\tau) = \frac{1}{N}\left(1 + \frac{\tau}{\tau_D}\right)^{-1}\left(1 + \frac{\tau}{\omega^2 \tau_D}\right)^{-1/2} \qquad \text{(equation 3)}$$

Where N is the number of particles in the observation volume and ω= l/r is the longitudinal to transverse radius ratio of the 3D Gaussian volume. If the diffusing species undergoes any other process having amplitude A and timescale τ_R that gives rise to additional fluorescence fluctuation, the modified correlation function can be written as[1]:

$$G(\tau) = \frac{1}{N}\left(1 + \frac{\tau}{\tau_D}\right)^{-1}\left(1 + \frac{\tau}{\omega^2\tau_D}\right)^{-1/2}\left(1 + A \cdot exp\left(-\frac{\tau}{\tau_R}\right)\right) \quad \text{(equation 4)}$$

We estimated the detection volume to be 0.6 fL using the equation[2],

$$V_{eff} = \pi^{\frac{3}{2}} r^3 \omega \quad \text{(equation 5)}$$

With the addition of DES, the refractive index and viscosity of the solution may change significantly in addition to the diffusion of the solute. We corrected the viscosity change by performing a control experiment at every experimental point, taking rhodamine-6G (R6G) as the fluorophore. R6G is a rigid molecule that is unaffected by DES. In this way, any change in its diffusion time through the detection volume will be exclusively because of the change in the medium viscosity. Using this information and the reported value of the diffusion coefficient of R6G in water[3] ($D_t = 4.14 \times 10^{-6}$ cm^2 s^{-1}) and the hydrodynamic radius of R6G (7.7 Å) in pH 7.4 buffer, the hydrodynamic radius of HSA can be calculated at every experimental point according to the following equation.

$$r_H^{HSA} = r_H^{R6G} \times \frac{\tau_D^{HSA}}{\tau_D^{R6G}} \quad \text{(equation 6)}$$

The change in the refractive index is compensated for by changing the objective collar position and setting it to have the highest G(0) and consecutively lowest τ_D value for each of the samples. In this way, we maintain the lowest detection volume.

Section S3: Translational diffusion of R6G in hydrated 0.5Ac\0.3Ur\0.2Sor DES and in same concentration constituent's solution

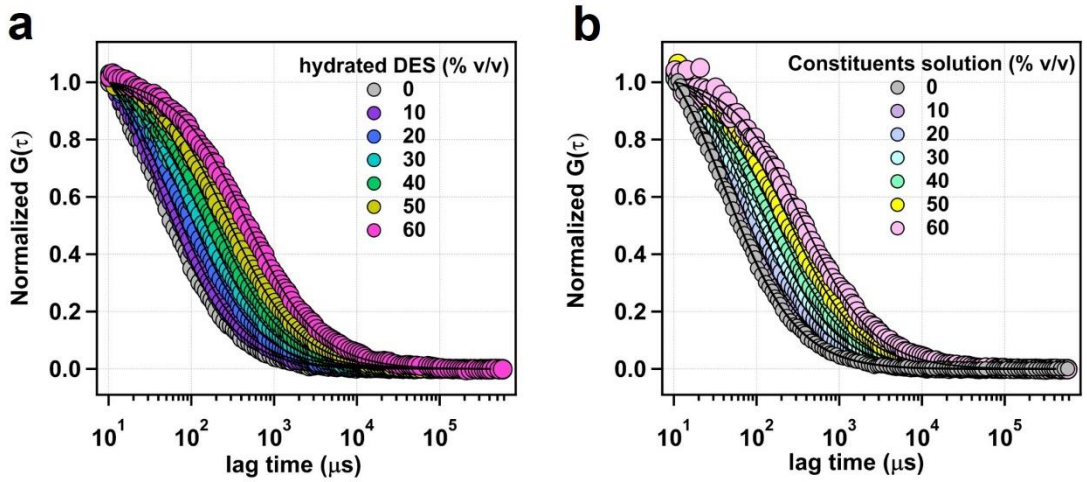

Figure S4. Normalized autocorrelation curve of R6G in presence of **(a)** hydrated 0.5Ac\0.3Ur\0.2Sor DES and (b) DES constituents' solution. Solid lines represent fitting by equation 3.

Section S4: Solvation dynamics of hydrated 0.5Ac\0.3Ur\0.2Sor DES with coumarin 343 (C 343) in the absence of protein using transient absorption spectroscopy

A: Time-resolved stimulated emission spectra

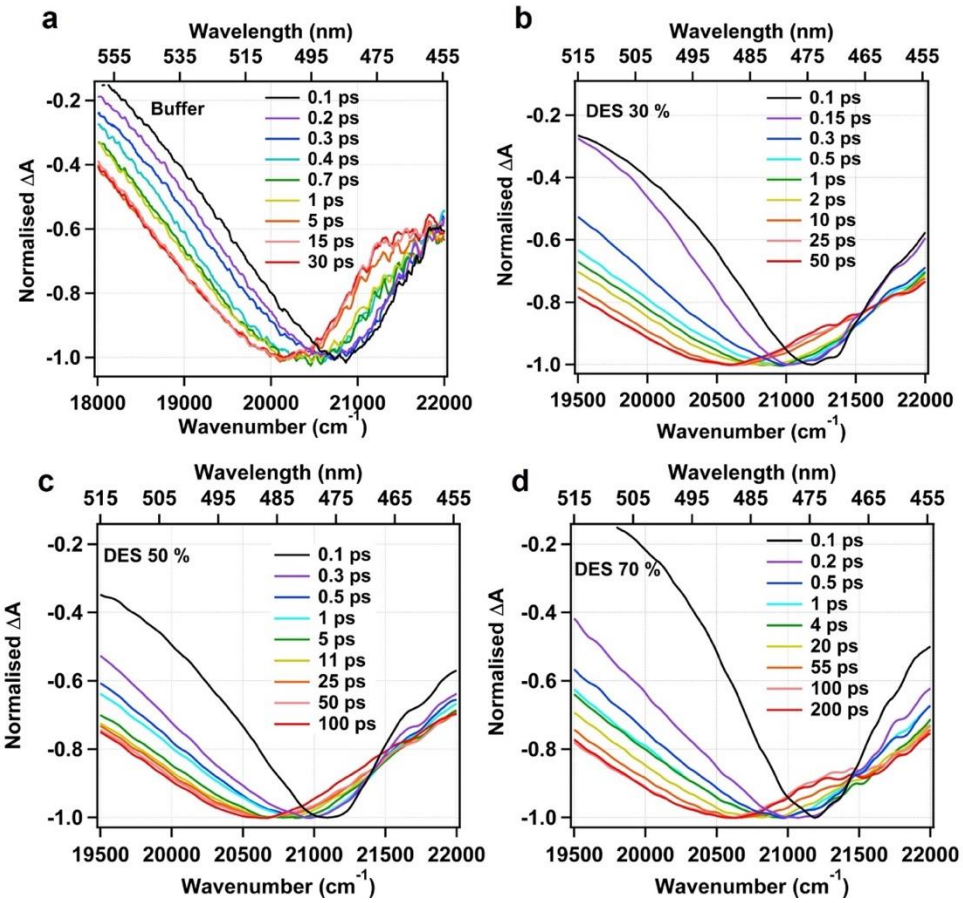

Figure S5. Time-resolved stimulated emission spectra of C 343 in (a) buffer, (b) 30% (v/v), (C) 50% (v/v), and (d) 70% (v/v) hydrated DES concentrations.

Table S2. Biexponential fitting parameters of the solvent response function, S(t), of C-343 in the presence of different concentrations of hydrated 0.5Ac/0.3Ur/0.2Sor DES

DES concentration	a_1(%)	τ_{S_1} (ps)	a_2 (%)	τ_{S_2} (ps)	τ_{avg} (ps)
0	49.6	0.19	50.4	1.41	0.80
10	49.3	0.13	50.7	1.30	0.72
20	43.2	0.16	56.8	2.46	1.47
30	50.4	0.18	49.6	4.32	2.23
40	56.4	0.15	43.6	4.62	2.10
50	54.3	0.16	45.7	7.91	3.70
60	58.0	0.15	42.0	22.2	9.41
70	49.6	0.15	50.4	37.3	18.85

Section S5: Time resolved emission spectra of CPM tagged HSA in presence of hydrated 0.5Ac\0.3Ur\0.2Sor DES

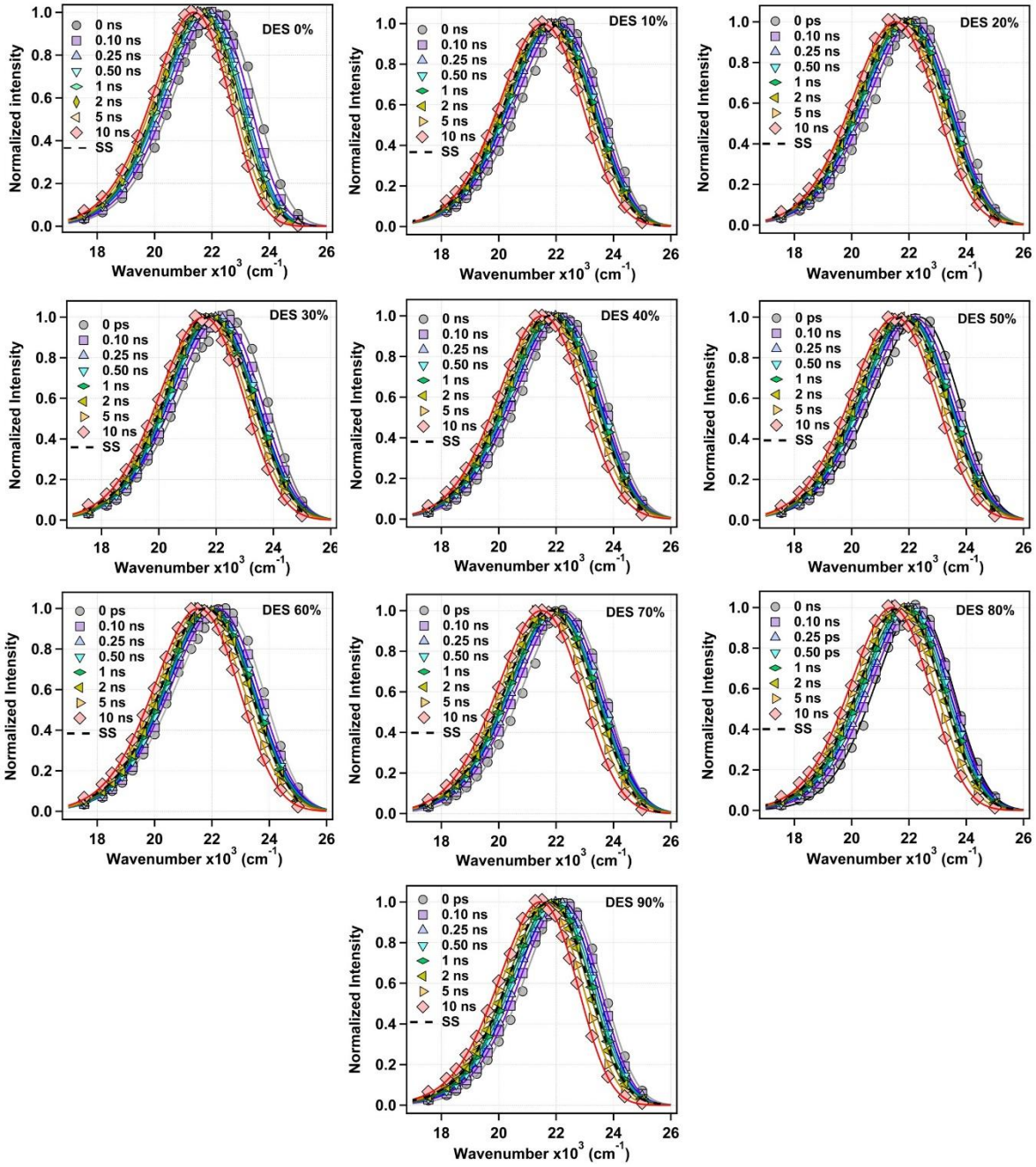

Figure S6. Time resolved emission spectra (TRES) of CPM labelled HSA with different degrees of hydrated (0.5Ac\0.3Ur\0.2Sor) DES. Black dashed line represents the steady state (SS) emission spectra of CPM labelled HSA at the respective DES concentration.

Section S6: Time resolved emission spectra of CPM tagged HSA in the constituent's solution of 0.5Ac\0.3Ur\0.2Sor DES

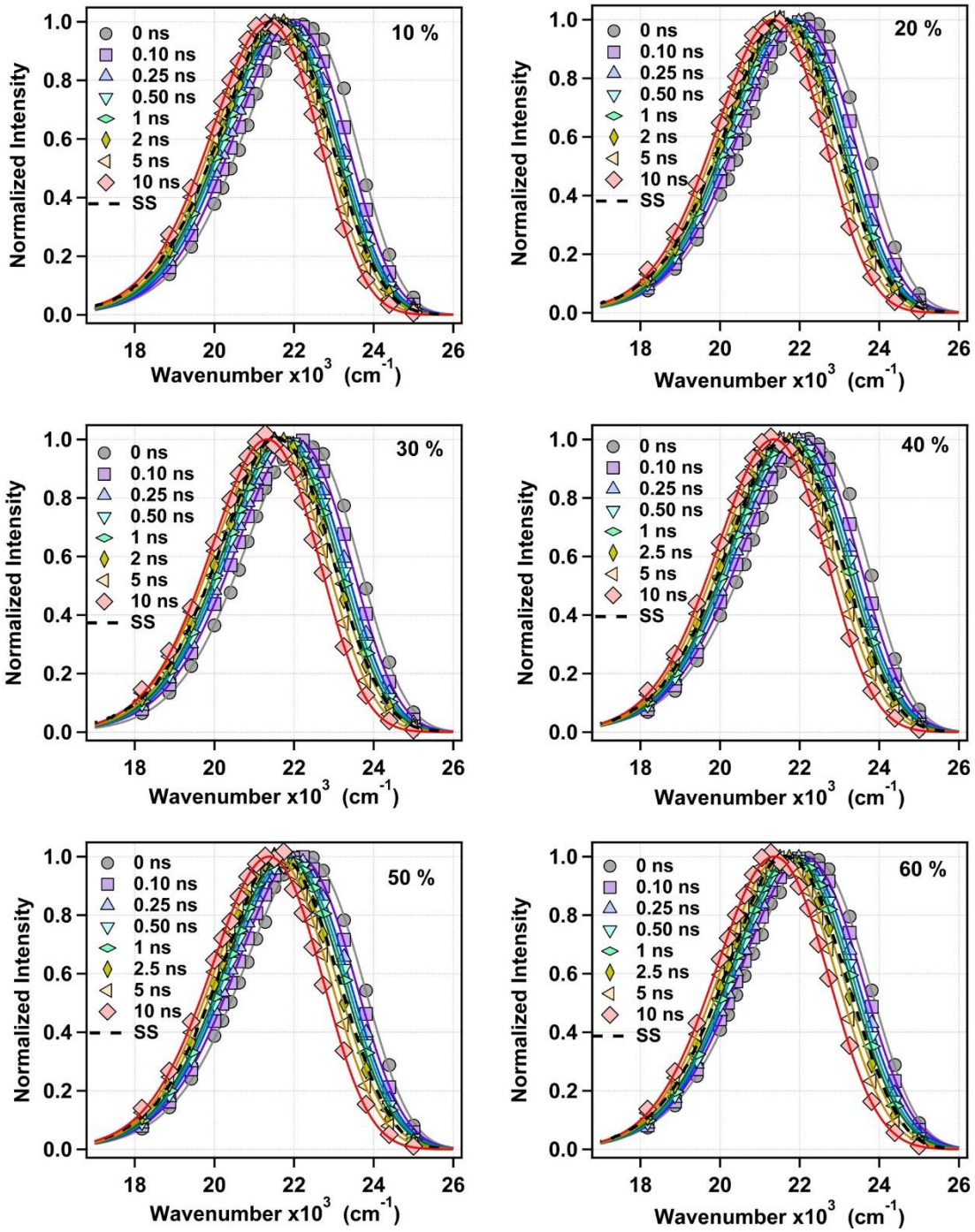

Figure S7. Time resolved emission spectra (TRES) of CPM labelled HSA in presence of different concentrations of constituent's solution of 0.5Ac/0.3Ur/0.2Sor DES.

Section S7: Structural alteration of HSA through steady state emission and FCS in presence of hydrated 0.5Ac\0.3Ur\0.2Sor DES

A: Steady-state emission data

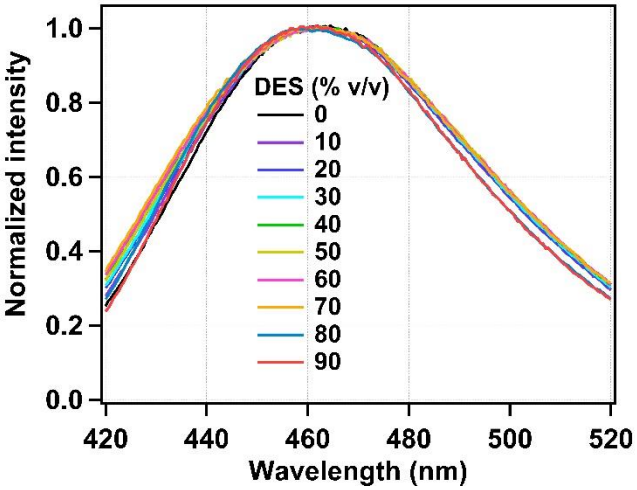

Figure S8. Intensity normalized emission spectra of CPM tagged to HSA in presence of hydrated 0.5Ac\0.3Ur\0.2Sor DES

B: FCS data

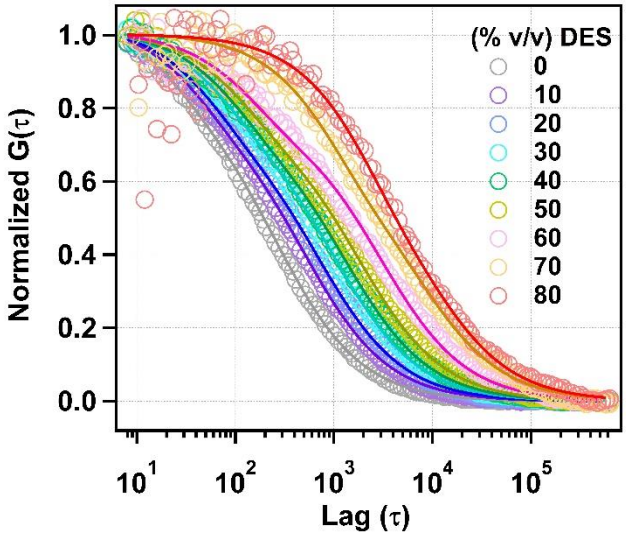

Figure S9. Normalized fluorescence intensity autocorrelation curve of TMR tagged HSA in presence of differently hydrated 0.5Ac\0.3Ur\0.2Sor DES

Section S8: Temperature dependent steady state emission study (thermal stability) of CPM tagged HSA in presence of hydrated 0.5Ac\0.3Ur\0.2Sor DES

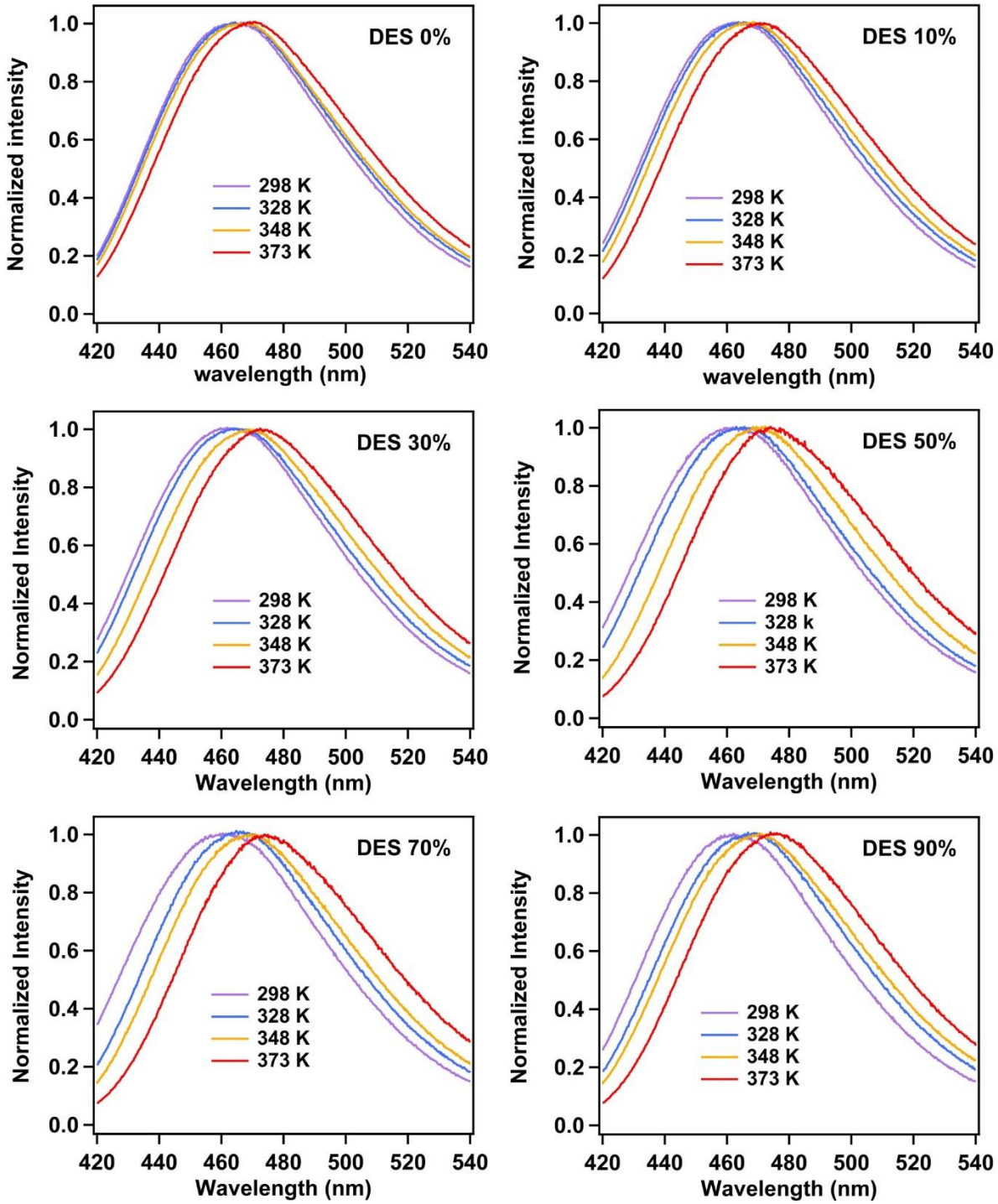

Figure S10. Representative intensity normalized temperature dependent emission spectra of CPM tagged to HSA in presence of differently hydrated 0.5Ac\0.3Ur\0.2Sor DES

Section S9: Temperature dependent steady state emission study (thermal stability) of CPM tagged HSA in the component's solution of 0.5Ac\0.3Ur\0.2Sor DES

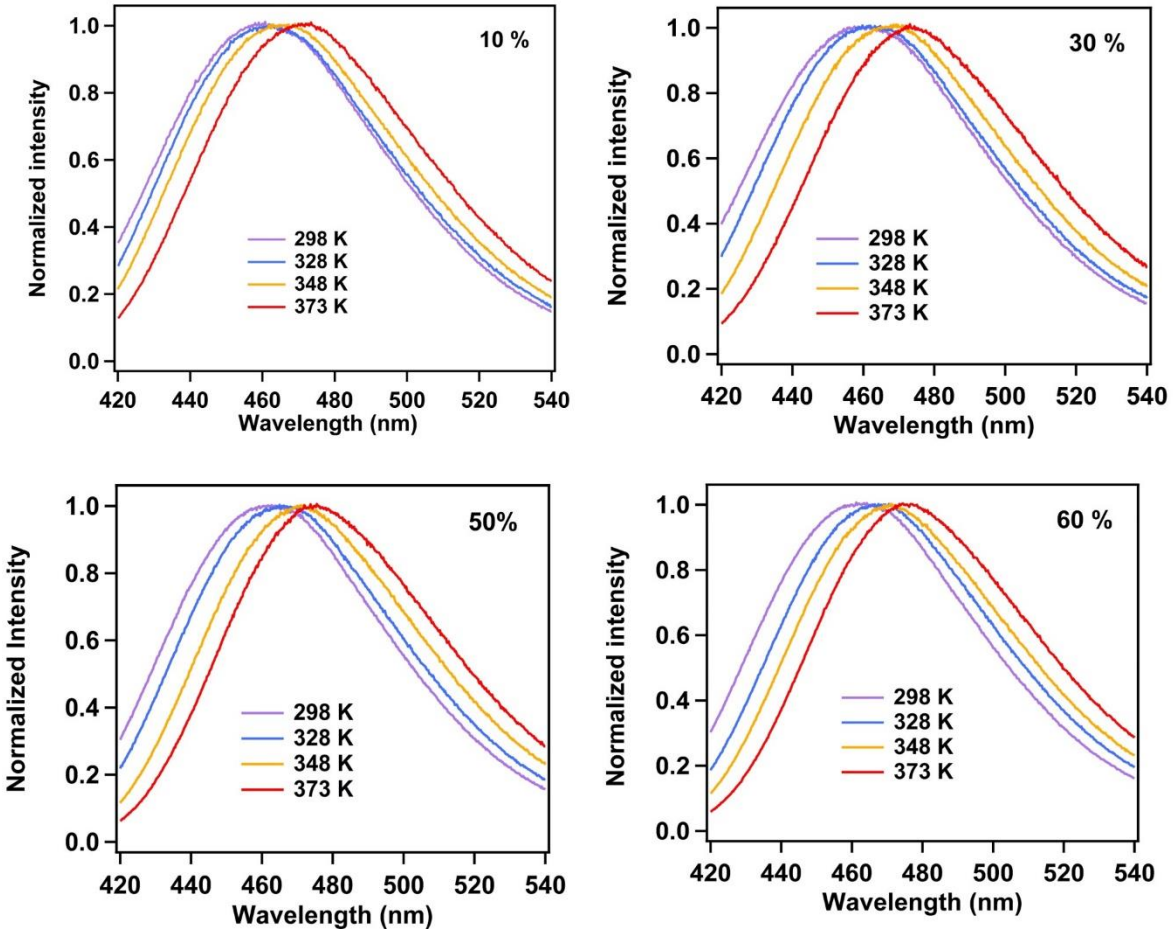

Figure S11. Representative intensity normalized temperature dependent emission spectra of CPM tagged to HSA in presence of solution of constituents of 0.5Ac\0.3Ur\0.2Sor DES

Section S10: Melting curves of CPM tagged HSA in the component's solution of 0.5Ac\0.3Ur\0.2Sor DES and comparison with same concentration hydrated DES

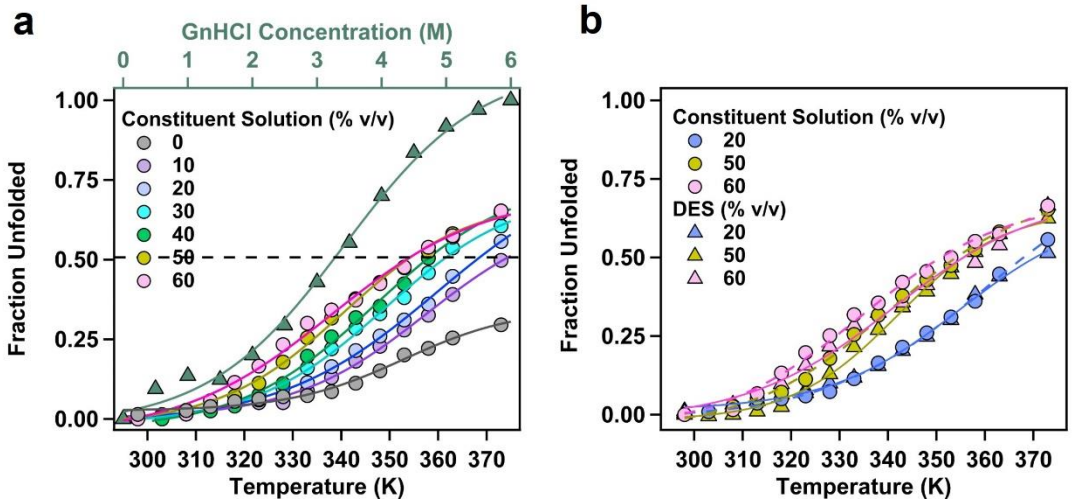

Figure S12. (a) Melting curves in terms of fraction unfolded of CPM-tagged HSA at different concentrations of constituent's solution in buffer. The solid/broken lines are the eye guides. Note that emission maxima in the presence of 6M GnHCl has been taken as the totally unfolded state in calculating fraction unfolded curves at each DES concentration. Variation of the fraction unfolded with increasing concentration of GnHCl (dark green) was plotted with respect to the similar colour coded top axis (dark green). (b) Comparison of melting curves of HSA in presence of similar concentrations of hydrated DES(circle and solid lines) and in its component's solution (triangle and broken lines).

References:

[1] T. Wohland, S. Maiti, R. Macháň, An Introduction to Fluorescence Correlation Spectroscopy, An Introduction to Fluorescence Correlation Spectroscopy. (2020). https://doi.org/10.1088/978-0-7503-2080-1.

[2] J.R. Lakowicz, Principles of fluorescence spectroscopy, Principles of Fluorescence Spectroscopy. (2006) 1–954. https://doi.org/10.1007/978-0-387-46312-4/COVER.

[3] C.B. Müller, A. Loman, V. Pacheco, F. Koberling, D. Willbold, W. Richtering, J. Enderlein, Precise measurement of diffusion by multi-color dual-focus fluorescence correlation spectroscopy, EPL. 83 (2008) 46001. https://doi.org/10.1209/0295-5075/83/46001.

[4] N. Das, T. Khan, N. Subba, P. Sen, Correlating Bromelain's activity with its structure and active-site dynamics and the medium's physical properties in a hydrated deep eutectic solvent, Phys. Chem. Chem. Phys. 23 (2021) 9337–9346. https://doi.org/10.1039/d1cp00046b.

[5] G. Bohm, R. Muhr, R. Jaenicke, Quantitative analysis of protein far UV circular dichroism spectra by neural networks, Protein Eng. 5 (1992) 191–195. https://academic.oup.com/peds/article/5/3/191/1535269.

[6] N. Das, E. Tarif, A. Dutta, P. Sen, Associated Water Dynamics Might Be a Key Factor Affecting Protein Stability in the Crowded Milieu, J. Phys. Chem. B. 127 (2023) 3151–3163. https://doi.org/10.1021/acs.jpcb.2c09043.